sRNA-mediated crosstalk between cell wall stress and galactose metabolism in *Staphylococcus aureus*

Maeliss Germain[1], Hugo Robin[1], Agnès Burel[2], Sébastien Massier[3] Nicolas Nalpas[4], Julie Hardouin[3,4], Philippe Bouloc[5], Astrid Rouillon[1], Svetlana Chabelskaya[1†]

[1]Inserm, BRM [Bacterial Regulatory RNAs and Medicine] - UMR_S 1230, 35033 Rennes, France.

[2]Microscopy Rennes Imaging Center (MRic) - UMS Biosit (FBI member (ANR-10-INBS-04))-University of Rennes.

[3]University of Rouen Normandie, INSERM US 51, CNRS UAR 2026, HeRacLeS-PISSARO, Normandie University, 76000 Rouen, France.

[4]University of Rouen Normandie, INSA Rouen Normandie, CNRS, Polymers, Biopolymers, Surfaces Laboratory UMR 6270, F-76000 Rouen, France.

[5]University Paris-Saclay, CEA, CNRS, Institute for Integrative Biology of the Cell (I2BC), 91198 Gif-sur-Yvette, France.

[†]corresponding author email: svetlana.chabelskaia@univ-rennes1.fr

ABSTRACT

Staphylococcus aureus is an opportunistic pathogen responsible for a wide range of infections in the human host. During infections, this bacterium is exposed to various stresses that target its cell wall, such as antibiotics, as well as environmental factors like acidification. *S. aureus* possesses effective regulatory systems to respond to the environmental stresses by expressing the factors necessary for its survival. Small RNAs (sRNAs) play a crucial role in bacterial adaptation processes by modulating bacterial physiology to respond to environmental stress. In this study, we describe RsaOI, a sRNA of *S. aureus* accumulated under acid stress conditions. We have shown that two-component system VraSR, involved in cell wall damage response, is also activated under acidic conditions and controls *rsaOI* expression. As a component of the VraSR-controlled regulon, RsaOI influences the survival of *S. aureus* under acid stress and affects its susceptibility to glycopeptide antibiotics. Our findings reveal that RsaOI targets *lacABCDFEG* operon, constituting the unique mechanism responsible for galactose metabolism in *S. aureus* named tagatose pathway. By antisense base pairing near the ribosome-binding site of *lacD*, RsaOI inhibits the expression of this gene, encoding tagatose-6-phosphate aldolase. This regulation disrupts the tagatose pathway, impairing galactose utilization in *S. aureus*. Furthermore, we demonstrated that disruption of the *lac* operon repression leads to significant alterations in the cell morphology and cell envelope structure. These findings highlight the role of RsaOI in the mediation between cell wall stress responses and specific metabolic pathway.

INTRODUCTION

Staphylococcus aureus (*S. aureus*) is a member of the commensal flora that can act as an opportunistic pathogen, responsible for both nosocomial and community-acquired infections (1). Its remarkable ability to cause a wide range of infections and establish successful colonization is largely due to its adaptability and resilience. *S. aureus* can survive and proliferate in various hostile environments within the human host, including acidic conditions (2). Such acidic microenvironments are commonly encountered on mucosal surfaces, in infected tissues where the immune response creates localized acidic conditions, and within phagolysosomes in the case of intracellular bacteria. To withstand these stresses, *S. aureus* employs a variety of adaptive mechanisms, including regulatory networks that allow rapid modulation of cellular processes essential for survival (2). One such adaptation involves reducing the permeability of the cell membrane and cell wall to protons by altering their charge composition. During acid stress, Gram-positive bacteria increase the expression of genes involved in cell wall modifications, such as the *cap* gene, linked to capsule biosynthesis, and the *dlt* operon, which adds positive charges to teichoic acids, enhancing resistance to acidic conditions (3–5). Another approach is the use of proton pumps such as the F_0F_1-ATPase, which pump excess protons out of the cell (6, 7). Additionally, bacteria increase the concentration of alkaline compounds within the cell to counteract the acidification of the cytoplasm. For this *S. aureus* increases the import of amino acids and osmolytes to maintain intracellular pH through decarboxylation reactions that consume protons (8, 9). Moreover, ammonia production is also promoted, either from urea through urease activity or via the arginine deaminase system (7, 10). Finally, energy metabolism and metabolic pathways are significantly reoriented. Respiration is favoured over fermentative metabolism to limit additional acidification of the environment (8).

Global transcriptomic analyses have offered provided insights into how *S. aureus* adjusts its gene expression profiles to adapt to acidic environments, revealing the complexity of its stress response mechanisms (5, 7, 11, 12). Despite these advances, the regulators that coordinate acid survival mechanisms remain only partially characterized. Studies focused on a small number of transcriptional regulators provide only fragmentary insights into the network, yet they hint at its complexity. For instance, transcription of urease, a crucial enzyme in acid stress responses, was shown to be controlled by global regulators, CcpA, CodY, and Agr (13). In addition, two-component systems (TCS), which integrate a signaling sensor kinase and a response regulator, play important roles in adapting to acidic stress. For example, the GraRS TCS has been shown to be involved in resistance to antimicrobial peptides under acidic conditions (14) and to enhance *S. aureus* survival within the acidified phagolysosomes of macrophages (15).

Although transcriptomic studies provide extensive information on acid stress responses, they often overlook post-transcriptional regulation. However, adapting to environmental changes often requires transcription factors to work in conjunction with post-transcriptional mechanisms mediated by small RNAs (sRNAs) (16, 17). Most sRNAs are RNA molecules between 50 and 500 nucleotides in length and play crucial roles in various cellular processes, especially under specific growth and stress conditions, enabling faster regulatory responses than transcriptional mechanisms alone (18). Typically, sRNAs act through antisense base pairing with the mRNA of their target genes (18–20). While numerous studies highlight the involvement of diverse protein regulators, the role of sRNAs in orchestrating these adaptive responses remains poorly understood, despite emerging evidence suggesting that sRNAs are essential for fine-tuning responses to environmental stressors.

In this study, we analyzed transcriptomic responses of *S. aureus* under acidic pH, with a focus on sRNA expression. Our analysis identified a notable sRNA, RsaOI (Srn1490_RsaOI_Teg47)(21), which exhibited a marked increase in expression under acidic conditions. We further investigated the regulatory mechanisms governing RsaOI expression and characterized its targetome. Our data reveal that the TCS VraSR, known for its role in cell wall stress response, is activated under acidic conditions and induces the expression of RsaOI. RsaOI targetome analysis identified that this sRNA inhibits the expression of *lacD*. The latter is part of the lactose operon which is responsible for lactose and galactose metabolism. These findings suggest that RsaOI functions as a regulatory mediator, linking cell wall stress responses with metabolic adjustments, particularly in coordinating lactose metabolism under acid stress. This crosstalk highlights a novel regulatory strategy by which *S. aureus* fine-tunes its metabolic priorities to optimize growth and survival in challenging environments.

MATERIAL & METHODS

Bacterial strains, plasmids and growth conditions

The strains and plasmids utilized in this study are detailed in Supplementary Table S1. Supplementary Table S2 lists all the primers used. Unless otherwise specified, *Staphylococcus aureus* strains were grown in Brain Heart Infusion medium (BHI, Oxoid) at 37°C with shaking (160 rpm), or on BHI agar (Oxoid) at 37°C. *Escherichia coli* DH5-α strains were grown in Luria-Bertani (LB) broth at 37°C with shaking (160 rpm) or LB agar plates at 37°C. For the maintenance of plasmids or resistance cassettes, antibiotics were used at the following concentrations: for *S. aureus*, erythromycin and chloramphenicol at 10µg/ml; for *E. coli*, ampicillin at 50µg/ml. The purified plasmids were used for the transformation in *S. aureus* RN4220 strain by electroporation shock. The φ80 phages prepared from RN4220 were then used to transduce plasmids in HG003 strains. pIMAYΔ*lacR* vector is a pIMAY (22) derivative containing the PCR-amplified *lacR* upstream and downstream sequences cloned by Gibson assembly (using primers from Supplementary Table S2) as described (23). The *lacR*

gene was deleted in *S. aureus* HG003 strain using pIMAY as described previously (23). Other *S. aureus* mutants were constructed by transducing the erythromycin resistance cassette from the Nebraska Tn mutant library USA300 (24) into the HG003 strain using φ80 phage.

To induce acidic stress, cells were grown for two or six hours in a LB medium supplemented with 100mM HEPES to maintain pH to 7. Cells were then divided, pelleted by centrifugation at 3000 rpm for 5 minutes, and resuspended in fresh LB medium buffered with HEPES to pH5 or pH7 for 30 minutes.

For metabolic tests**,** *S. aureus* strains WT, Δ*rsaOI* (both carrying pICS3 plasmid), or Δ*rsaOI* complemented strain (carrying pICS3-P*amiA-rsaOI* plasmid), were cultured at 37°C in Luria-Bertani (LB) or NZM broth and then diluted to 1:100 ratio in fresh media. When necessary, the media were supplemented with glucose or galactose at a concentration of 11mM, and HEPES at 100mM. Growths were measured by Biotek microplates reader.

Construction of *gfp*-reporter transcriptional and translational fusions

pCN33 and pCN38-based vectors containing *gfp*-reporter fusions were constructed using primers from Supplementary Table 2. *gyrB* sequence of pCN33-*PtufA-gyrB-gfp* vector was replaced for 5 lacD sequence to produce pCN33-*PtufA-lacD-gfp*. For the pCN38-*PrsaOI-gyrB-gfp* construction, *rsaOI* promoter region (-99 nucleotides to +39 after the +1 transcription) was amplified from *S. aureus* HG003 genomic DNA by PCR. The *rsaOI* promoter fragment was placed instead of P*tufA* promoter of vector pCN33-*PtufA-gyrB-gfp*. All cloning experiments were performed with Gibson Assembly Master Mix (New England Biolabs). The reactions were then transformed into *E. coli* DH5-α by heat shock at 42°C.The constructs were confirmed by DNA sequencing, and then electroporated into RN4220 before being transduced into HG003 or its derivatives using bacteriophage Φ80. When necessary, *S. aureus* HG003 strain was used to co-transform the *lacD-gfp* fusion vector with the *rsaOI* expressing plasmid. Cultures of these co-transformed S. aureus strains were grown at 37°C in LB or BHI supplemented with 10 μg/ml chloramphenicol and erythromycin. Fluorescence and OD_{600} measurements were driven by Biotek microplates reader as previously described (25). To induce *rsaOI* expression, cells were grown in LB medium for two hours, then divided, with one sample receiving 10µl of HCl 37% per 10ml of culture.

Induction of acidic stress for acid susceptibility tests and proteomic studies

To induce *rsaOI* expression by acidic pH, cells were grown for two hours in a LB medium supplemented with 100mM HEPES to maintain pH to 7. Cells were pelleted by centrifugation at 3000

rpm for 5 minutes and resuspended in a fresh LB medium buffered with HEPES to pH5 for an additional 2 hours. After stress induction, cells were collected and pelleted by centrifugation for proteomic studies or plated on BHI agar plates for CFU counting.

Antibiotic susceptibility tests

Ten-fold serial dilutions of overnight cultures of WT HG003, Δ*rsaoi* or complemented strain (Δ*rsaOI/p-rsaOI*) were plated and incubated for 24 hours at 37°C on TSA or TSA supplemented with 1µg/ml vancomycin. For the spot population analysis profile assay (spot PAP), five microliters of each dilution were dropped on TSA or TSA supplemented with 1µg/ml vancomycin, and then incubated for 24°C at 37°C. Dilutions were deposed from top to the most-concentrated (without dilution), to the dilution 10^{-6}.

RNA-sequencing method

Total RNA extraction was performed as previously described (26) on three independent replicates. RNA quality was then evaluated on a High Sensitivity RNA Screen Tape chip (Agilent). rRNA depletion, cDNA library and sequencing were performed by Genewize® platform using their Strand-Specific RNA-seq protocol. The resulting FASTQ raw data were imported into the Galaxy web platform, using the public server at https://usegalaxy.eu/ for data analysis. Reads were cleaned using Trimmomatic (version 0.39) and mapped to the *S. aureus* NCTC8325 reference genome, including the file containing sRNA genes annotated for NCTC8325 (https://srd.genouest.org/browse/NCTC8325), using the BWA (version 0.7.18) algorithm. Counting files were generated with HTseq-count (version 2.0.5) and differentially expressed transcripts were identified using DEseq2 (version 1.40.2). Transcripts and genes with a *p-value* < 0.05 and a fold change > 2 were considered significantly differentially expressed across biological replicates.

Preparation of samples for proteomic studies

Bacteria were prepared as described in the section on acidic stress induction. After pH induction, samples were centrifuged at 4500 rpm for 15min at 4°C, and washed twice with cold PBS. The pelleted cells were then resuspended in 500µl of Tris-HCl (pH8) supplemented with a mini cOmplete (Roche) protease inhibitors cocktail, 2U of DNAse, 2U of RNAse. Bacteria were lysed using a Fast-Prep system, then centrifuged for 10min at 12,000 rpm at 4°C. Protein concentration was measured using a Qubit assay, and 500µg were precipitate with 17,5% TCA overnight at 4°C. The samples were centrifuged at 9000 rpm for 15min at 4°C, and supernatant was discarded. The pellets were rinsed

twice with 2 volumes of cold acetone (100%), and mixed by inversion, followed by the same centrifugation as described before. Samples were dried in a speed vacuum and stored at -80°C.

Proteins solubilization and quantification

TCA-precipated proteins were then solubilized in 200 µL of R2D2 denaturing buffer (7 M urea, 2 M thiourea, tri-N-butylphosphine (TBP) 2 mM, dithiothreitol (DTT) 20 mM, 0.5% (w/v) 3-(4-heptyl)phenyl-3-hydroxypropyl)dimethylammoniopropanesulfonate (C7BzO), 2% (w/v) 3-[(3-cholamidopropyl)dimethylammonio]-1-propanesulfonate hydrate (CHAPS)) and sonicated for 30 sec. Protein concentrations were evaluated by Bradford analysis (Bio-Rad). Samples were stored in aliquots (30 µg) at −20 °C until further use.

Protein Digestion

Twenty-five micrograms of proteins were mixed with sodium dodecyl sulfate (SDS) loading buffer (62 mM Tris-HCl pH 6.8, 20% glycerol (v/v), 0.04% bromophenol blue (w/v), 0.1 M DTT, SDS 4% (w/v)) heated at 95 °C for 5 min, and then loaded onto a large SDS-PAGE stacking gel 7%. An electrophoresis was performed (10 mA, 2 hours) to concentrate proteins. After migration, gels were stained with Coomassie Blue G250 and destained (50% ethanol (v/v) and 10% acetic acid (v/v)). The revealed protein band was excised, completely destained and washed three times with water. Samples were then reduced with 10 mM Dithiothreitol (DTT) for 1 hour at room temperature and alkylated with 15 mM Iodoacetamide for 45 minutes in the dark. Gel bands were treated with 50% acetonitrile (ACN)/50% ammonium bicarbonate 10 mM, pH 8 (2 times, 5 min) and dried with 100% ACN (3 times, 10 min). Then, proteins were digested with trypsin (1 µg per band, ratio of 1:25), overnight at 37 °C, in ammonium bicarbonate 10 mM, pH 8. Peptides were extracted with 100% ACN (3 times, 10 min) and then dried using a Speedvac concentrator (SPD111V, Thermo Fisher Scientific) and stored at −20 °C. For each type of bacteria (wild type and mutants), five biological replicates were carried.

LC-MS/MS analysis

Peptides were solubilized in 0.1% formic acid (FA) (v/v) and quantified using Pierce quantitative colorimetric peptide assay (Thermo scientific). Peptides (0.2 µg) were subjected to quantitative LC-MS/MS analysis on a high-resolution Orbitrap Eclipse Tribrid mass spectrometer coupled to a Proxeon Easy nLC 1200 (Thermo Scientific). Samples were injected onto an enrichment column (Acclaim PepMap C18, 2 cm × 75 µm, 100 Å, Thermo Scientific). The separation was performed with an analytical column needle (Acclaim PepMap C18, 25 cm × 75 µm, 2 µm, 100 Å, Thermo Scientific).

The mobile phase consisted of H2O/0.1% formic acid (FA) (buffer A) and CH3CN/FA 0.1% (80/20, buffer B). Tryptic peptides were eluted at a flow rate of 300 nL/min using a three-step linear gradient: from 2 to 40% B over 123 min, from 40 to 100% B in 1 and 10 min at 100% B. The mass spectrometer was operated in positive ionization mode with capillary voltage and source temperature set at 1.9 kV and 275 °C, respectively. The samples were analyzed using HCD (higher-energy collision dissociation) method. The first scan (MS spectra) was recorded in the Orbitrap analyzer (R = 120,000) with the mass range m/z 400–1800. Then, 20 scans were recorded for MS2 experiments. Singly charged species were excluded for MS2 experiments. Dynamic exclusion of already fragmented precursor ions was applied for 30 s, and an exclusion mass width of ± 10 ppm. Peptide isolation was achieved in the quadrupole with an isolation window of 1.6 m/z. Fragmentation occurred with a HCD collision energy of 28%. Daughter ions were analyzed in the Orbitrap with a resolution of 15,000. The maximum injection times were 30 ms and 22 ms for MS and MS2 analyses, respectively. All measurements in the Orbitrap analyzer were performed with on-the-fly internal recalibration (lock mass) at m/z 445.12002 (polydimethylcyclosiloxane).

Protein Quantification

Raw data were imported in Progenesis LC-MS/MS software (Waters, ver. 4.1, UK). A 2-dimensional map was generated for each sample (retention time versus *m/z* ratio). The spots present on the 2D maps were then aligned. Monocharged ions and those with a charge greater than 5 were excluded from the analysis. MS/MS spectra from selected peptides were exported for peptide identification with Mascot (Matrix Science, ver. 2.2.04) against the S. aureus NCTC 8325 database available online (https://www.ncbi.nlm.nih.gov/datasets/taxonomy/93061/). Database searches were performed with the following parameters: 1 missed trypsin cleavage site allowed; variable modifications: carbamidomethylation of cysteine and oxidation of methionine. Mass tolerances for precursor and fragment ions were both set at 5 ppm. Then, Mascot search results were imported into Progenesis. Peptides with an identification score greater than 13 are retained. Proteins identified with less than 2 peptides were discarded. For each condition (Wild type and mutants), the total cumulative abundance of the protein was calculated by summing the peptides abundances. The software compared the intensity of the isotopic mass of all the ions for each condition. The abundances were normalized to perform a relative quantification of each protein between the conditions.

Statistical analyses of proteomic data

Significance analyses of differentially regulated proteins were performed with Perseus software (version 2.0.10.0.). Proteins normalized abundance (from Progenesis) were transformed to log10

space. Significantly regulated proteins between the different strains (Wild type, Mutant and complemented) were identified by two sample t test with a *p-value* ≤ 0.05 and volcano plot was generated.

Functional annotation and functional enrichment analysis

The proteins were functionally annotated via NCBI, UniProt and Kyoto Encyclopedia of Genes and Genomes (KEGG) functional resources and added to the Perseus software. The significantly up- and down-regulated proteins from the three different comparisons were tested for functional enrichment based on KEGG pathways by using the Fisher's exact test. Annotation terms were considered significant on the basis of an enrichment factor ≥ 1, an intersection size > 2 and a p-value ≤ 0.2.

Microscopy

S. aureus HG003 WT, *ΔlacR*, *ΔlacC*, were cultured in BHI during 6 hours. Cell pellets were obtained after cell suspension centrifugation (1,000–3,000g for 5 min). Samples were fixed for 2 h with 2.5% glutaraldehyde in 0.1 M cacodylate buffer (pH 7.2), rinsed, fixed again for 2 h with 1% OsO4 in the same buffer, and washed. S. aureus Newman samples were embedded in 2% agar and dehydrated in a graded series of increasing ethanol concentrations (50, 70, 90, and 100% v/v). After the dehydration, the samples were embedded in conventional Epon resin (EMS, 1420) and then polymerized at 60°C for 48 h in blocks. Resins blocks were then sectioned into 80-nm sections using ultramicrotome LEICA UC7 (Leica, Wetzlar, Germany). These sections were mounted on copper grids stained and were observed using a JEM-1400 Electron Microscope (JEOL Ltd, Tokyo, Japan) at an accelerating voltage of 120 kV and equipped with an Orious® SC1000 camera (Gatan-Ametek, Pleasanton, USA). The cell size measurements were carried out by TEM using Fijy software on two batches of culture and on 50 different bacterial cells for each culture.

RNA extractions, Northern blots, RNA half-life and RT-qPCR

The cells were collected and pelleted for 10 min at 4°C, at 4500 rpm, then resuspended in RNA lysis buffer consisting of 0.5% SDS, 20 mM sodium acetate, 1 mM EDTA, pH 5.5. Total RNA extraction was performed as previously described (27). Northern blot assays were conducted following established protocols (27). Membranes were hybridized with specific 32P-labeled probes (Supplementary Table S2) in ExpressHyb solution (Ozyme) and washed according to recommendations from manufacture. The membranes were exposed and scanned with Typhoon FLA 9500 scanner (GE Healthcare). Image quantification was carried out using ImageQuant Tool 7.0. To

determine the half-life of sRNA, rifampicin (20 mg/ml) was employed as the standard treatment to halt transcription. Approximately 4 ml of each strain was collected prior to and at 2, 5, 10, 20, 30, 40, and 60 minutes after rifampicin addition. These samples were centrifuged, and the pellets were frozen in liquid nitrogen and subsequently stored at -80°C for total RNA extraction. For quantitative real-time PCR (qRT-PCR), the total RNA extraction samples were treated with the DNase I Amplification Grade Kit (Invitrogen) to remove any residual DNA. cDNA preparations and qRT-PCR experiments were conducted as previously described (23), with the *gyrB* gene serving as the normalization control.

In vitro transcription, RNA labeling and gel retardation assays

Gel-shift assays were performed as described in (23). RNAs were synthesized from PCR-generated DNA using MEGAscript T7 kit (Ambion). The transcription template was amplified from HG003 genomic DNA and forward primers included T7 promoter sequences (Supplementary Table S2). Then, RNAs were labeled at 5′-end using [γ-32P] ATP (Amersham Biosciences) and T4 polynucleotide kinase (Invitrogen). Both labeled and unlabeled RNAs were purified on a 5% acrylamide-urea gel, eluted in elution buffer (20 mM Tris-HCl, pH 7.5; 250 mM NaCl; 1 mM EDTA; 1% SDS) at 37°C. The RNA was then ethanol-precipitated, quantified using a Qubit fluorometer (Thermo Fisher Scientific), and stored at -80°C. Gel-shift assays were conducted as outlined in (23). The RNAs were denatured in a solution of 50 mM Tris/HEPES (pH 7–7.5) and 50 mM NaCl for 2 minutes at 80°C, followed by refolding for 10 minutes at 25°C upon the addition of MgCl□ to a final concentration of 5 mM. Reactions were carried out in a buffer containing 50 mM Tris-HCl (pH 7.5), 50 mM NaCl, and 5 mM MgCl□ for 20 minutes at 25°C. Approximately 0.05 pmoles of labeled RsaOI or RsaOI-del were incubated with varying concentrations of *lacD* mRNA. The samples were supplemented with 10% glycerol and loaded onto a native 4% polyacrylamide gel containing 5% glycerol. The gels were subsequently dried and visualized using a Typhoon FLA 9500 scanner (GE Healthcare).

RESULTS

Transcriptome analysis of *S. aureus* under acid conditions reveals differently expressed *srna* genes

To identify sRNAs potentially involved in adaptation to a low pH environment, we performed RNA-seq analysis, comparing the transcriptome profiles of the HG003 strain under neutral (pH 7) and acidic (pH 4) conditions. For this purpose, total RNA was extracted from two HG003 cultures in the exponential growth phase, either maintained at neutral pH or exposed to acidic stress for 30 minutes, as outlined in the Materials and Methods.

Several genes identified as part of the acid stress response regulon showed increased expression (Supplementary Table 3). For instance, the *ure* operon encoding urease subunits A, B and C (*ureA*, *ureB* and *ureC*), which plays a role in maintaining intracellular pH, was upregulated (13). Urease activity is known to be the major acid-resistance mechanism (2). Additionally, the *kdpDE* operon, which encodes a two-component system involved in both acid and osmoprotection, was stimulated (28). Genes associated with histidine import and metabolism, essential for growth at low pH, were also upregulated (8). In agreement with previous studies on sudden inorganic stress, we observed a general reduction in the expression of ribosomal protein genes, and pyrimidine ribonucleotide biosynthesis pathway, which likely reflects the lowered growth rate after acidification (12).

In this report, we focused specifically on sRNA expression (Supplementary Table 4). Among the genes affected by low pH, *rsaOI* showed one of the most significant responses, with acidic conditions leading to more than a 14-fold accumulation of RsaOI (Figure 1A and Supplementary Table 4).

rsaOI expression is triggered by low pH, improving survival in acidic stress conditions

RsaOI is approximately 250 nucleotides (NT) long and represents the longest sRNA that we previously identified in strain N315 (Bohn et al., 2010). Using RACE (rapid amplification of cDNA ends), we mapped the 5'-end of *rsaOI* from HG003 strain to position 565901 in the NCTC8325 genome, which corresponds to the location identified previously for the N315 strain (29). The *rsaOI* gene is present in all analyzed *S. aureus* strains, exhibiting 100% sequence conservation across isolates (Supplementary Figure 1). Moreover, this sRNA is also found in other staphylococcal species, including *Staphylococcus schweitzeri* (coagulase-positive) and *Staphylococcus argentus* (coagulase-negative) with a variable sequence conservation (98,4 to 95,7% sequence identity respectively) (Supplementary Figure 1). In *S. aureus* and related staphylococcal species, compensatory mutations confirm that the last 30 nucleotides of RsaOI form a hairpin structure, which likely functions as a rho-independent transcription terminator (30). Moreover, in HG003 strain, *rsaOI* has its own promoter and transcription terminator, with no open reading frame on the opposite strand. This sRNA can therefore be classified as a *bona fide* sRNA (31). *rsaOI* gene is located between *proP* gene, encoding for an osmolyte transporter that facilitates bacterial adaptation to osmotic stress (32) and operon *vraABC* involved in fatty acid metabolism, and shown to be-upregulated in staphylococcal strains with increased resistance to vancomycin (33)(Figure 1B).

To validate and expand upon the results obtained from the RNA-seq analysis, we conducted a detailed examination of the effect of pH range on *rsaOI* expression using Northern blot and RT-qPCR analyses. We showed that the increase in RsaOI levels correlates with a decrease in the pH of medium: the highest accumulation of RsaOI was observed at pH 5 and 4, corresponding to 200-fold and 400-

fold increases, respectively, compared to RsaOI levels at pH 7 (Figure 1C and Supplementary Figure 2). This supports the low pH-dependent expression of *rsaOI*.

Previously, we demonstrated that in the N315 strain, *rsaOI* expression increased significantly during the stationary growth phase in nutrient-rich media, such as BHI (29). We compared the *rsaOI* expression profiles in three other reference strains (HG003, Newman, and USA300) and found that this expression pattern was conserved across all strains tested (Supplementary Figure 3A and 3B). To determine whether such increase in RsaOI levels was due to acidification of the medium when glucose is consumed during bacterial growth (5) or other factors, we analyzed *rsaOI* expression in LB medium with or without glucose, and under buffered pH conditions. In stable neutral pH conditions, glucose did not induce *rsaOI* expression. However, without pH buffering, glucose caused an acidification of the media, which led to the gradual increase in RsaOI levels (Supplementary Figures 4A and 4B). These findings demonstrate that *rsaOI* expression is induced not only by sudden acidic stress but also by a gradual, mild decrease in pH during growth. We also evaluated *rsaOI* expression under various stress conditions that bacteria are likely to encounter during infection and found that the only condition that significantly stimulates its expression is the acidic stress induced either by inorganic (HCl) or organic (Acetic acid) acids (Supplementary Figure 5).

We further investigated the role of RsaOI in *S. aureus* acid resistance. To assess this, HG003 wild-type (WT) and *rsaOI* deleted (Δ*rsaOI*) strains were exposed to acid stress at pH5, followed by plating to measure viability. Additionally, the *rsaOI* deletion was trans-complemented with high copy plasmid pICS3-*rsaOI*, expressing a wild-type copy of the *rsaOI* gene under control of its native promoter (Δ*rsaOI/p-rsaOI*) (Figure 1D). Colony-forming unit (CFU) counts revealed that *rsaOI* expression significantly improved survival rates compared to the Δ*rsaOI* strain (Figure 1E).

RsaOI expression is affected by envelope stress and regulated by VraSR two component system

To explore the mechanism underlying RsaOI accumulation we tested whether the increase in *rsaOI* expression under acidic conditions was due to its promoter activation. For this, we constructed a plasmid with GFP (Green Fluorescent Protein) under control of *rsaOI* promoter (pCN38-P*rsaOI-gfp*). As a control, a plasmid with GFP regulated by the *tufA* promoter was employed (pCN38-P*tufA-gfp*). Acidic conditions did not affect *tufA* promoter activity but did enhance the fluorescence associated with the *rsaOI* promoter (Figure 2A). To further validate these findings, we created a plasmid with *rsaOI* driven by a constitutive promoter *amiA* (pICS3-*PamiA-rsaOI*). While a decrease in pH did not impact RsaOI levels when *rsaOI* was under the control of the constitutive promoter, it did induce *rsaOI* expression when regulated by its native promoter (pICS3-*rsaOI*) (Supplementary Figure 6A). Additionally, we found that the decrease in pH does not affect RsaOI stability (Supplementary Figure

6B). Taken together, these results indicate that the increase in RsaOI levels under acidic conditions is driven by enhanced *rsaOI* promoter activity.

To identify the factor responsible for RsaOI accumulation under acidic conditions, we tested various mutant strains lacking specific transcription regulators, two-component systems (TCS), and sigma factor to evaluate their roles in *rsaOI* expression. We found that, as in the wild-type strain, acidic stress induced *rsaOI* expression in all tested mutants, except for the *vraR* mutant strain (Figure 2B). RsaOI accumulated under low pH conditions in wild-type strain, but not in *vraR* mutant, indicating the role of VraR in regulation its expression (Figure 2C). The VraR is response regulator of the VraSR (VraR/VraS) two-component system that regulates the staphylococcal response to disruptions in cell wall synthesis (34). This TCS was initially identified for its role in vancomycin resistance (35). Interestingly, previous studies have reported that expression of *rsaOI* was also increased in the presence of vancomycin, but the regulatory network involved was not identified (36, 37).

To test whether acidic stress activates the VraSR system, we evaluated the expression of *vraX* and *cwrA* genes, which are directly regulated by VraSR (38, 39). In accordance with transcriptomic data (Figure 1A), the expression of both, *vraX* and *cwrA*, was upregulated under acidic stress in wild-type HG003 strain (Supplementary Figure 7A and B). However, the expression of both genes was strongly downregulated in a *vraR* mutant (Supplementary Figure 7A and B). Those data indicate that *cwrA* and *vraX* are part of an acid stress regulon directly regulated by VraSR TCS. Additionally, we observed that acidic conditions slightly led to higher *vraSR* mRNA levels, consistent with findings previously reported by (12)(Supplementary Figure 7C).

To confirm that the regulation of *rsaOI* by VraSR TCS occurs *via* its promoter, HG003 wild-type strain and *ΔvraR* mutant were transformed by plasmid containing GFP reporter driven by the *rsaOI* promoter (pCN38-P*rsaOI-gfp*). No induction of fluorescence under acidic condition was observed in *ΔvraR* mutant, comparing to wild type strain, demonstrating that VraR stimulates the activity of *rsaOI* promoter (Figure 2D). Altogether, our results demonstrate that the VraSR two-component system induces the transcription of *rsaOI* in response to a decrease in external pH (Figure 2E).

VraSR recruitment and accumulation during short-term stress, resulting in an important increased expression of *vraX*, *cwrA*, and *rsaOI*. Taken together, these data demonstrate that in addition to responding to cell wall stress caused by previously reported cell wall-damaging agents (40), VraSR mediates response to low acidic growth conditions (Figure 2E).

RsaOI impacts *S. aureus* susceptibility to glycopeptide antibiotics

Since *rsaOI* was identified as part of the regulon of VraSR, a TCS, mobilized in response to cell wall stress and involved in resistance to cell wall active-antibiotics, we investigated whether RsaOI affects

S. aureus susceptibility to glycopeptide antibiotics. For this, we compared the *rsaOI* mutant strain and its parental wild-type strain HG003 for susceptibility to vancomycin, antibiotics from the glycopeptide family. Additionally, *rsaOI* deletion was trans-complemented with a plasmid pICS3-*rsaOI*. While no differences in growth were observed between the strains in the absence of vancomycin, the loss of *rsaOI* led to improved growth in the presence of the vancomycin, compared to the wild-type strain (Figure 3A and 3B). Complementation of the *rsaOI* deletion restored the reduced growth in the presence of vancomycin, confirming that RsaOI contributes to *S. aureus* susceptibility to this antibiotic. Similar results were obtained using a spot Population Analysis Profile assay (spot PAP), which allows rapid, sensitive and reproducible qualitative and quantitative testing of antibiotic resistance (Supplementary Figure 8)(41). Altogether, these fascinating features of RsaOI prompted us to investigate its targets and to elucidate the regulatory mechanism involved.

Identification of protein levels affected by RsaOI

To identify RsaOI-dependent changes in the abundance of individual proteins, we analyzed by quantitative proteomics which protein levels are affected by RsaOI expression. For this purpose, we compared the proteome of HG003 wild-type (WT), *ΔrsaOI*, and *ΔrsaOI* complemented with the pICS3-*rsaOI* vector. To ensure *rsaOI* expression from its native promoter in the HG003 WT and complemented strains, bacteria were grown under low pH conditions (Supplementary Figure 9A). From 2,573 annotated putative proteins in *S. aureus* NCTC 8325 (taxid: 93061) strain (42), 1,112 proteins were identified in HG003 wild-type, 1,012 in *ΔrsaOI* and 996 in *rsaOI* complemented strains. Tryptic peptides were analysed by nLC-MS/MS (n = 4 per conditions). We performed a functional enrichment analysis based on the significantly up- or down-regulated proteins in comparison *ΔrsaOI*/p vs WT/p, and *ΔrsaOI*/p vs *ΔrsaOI*/*p-rsaOI*. Overall, carbon metabolism proteins were upregulated in the *ΔrsaOI* strain compared to the WT or *rsaOI* complemented strains (Supplementary Figure 9B and 9C). For example, among these proteins, we found Fda (Fructose-1,6-bisphosphate aldolase) involved in glycolysis, PckA (PEP carboxylase) in gluconeogenesis, and SucA (2-oxoglutarate dehydrogenase E1 component) in the TCA cycle, as well as LacD (Tagatose 1,6-diphosphate aldolase) part of galactose metabolism.

Focusing on proteins with differential abundance between deletion strain *ΔrsaOI*/p and complemented strain *ΔrsaOI*/p-*rsaOI* using *t*-test (*p-value* ≤ 0.05), we highlight that a total of 389 proteins were significantly differentially regulated, including 144 proteins with a fold change greater than 2 (Figure 4A and Supplementary Table 5). Notably, the transcriptional regulator of RsaOI, VraR, was found to be less abundant in the strain expressing *rsaOI*. The inhibition of VraR protein levels is particularly interesting given the significantly reduced survival of a strain expressing *rsaOI* in the presence of glycopeptides. Focusing on proteins involved in metabolic pathways, we identified LacD as another

protein less abundant in the strain expressing the sRNA *rsaOI* (Figure 4A). This finding could be relevant in light of the impact of metabolism on medium acidification.

Integration of experimental data and computational prediction to highlight direct targets of RsaOI

The effect of sRNA on the abundance of specific proteins can also occur indirectly through its influence on regulatory proteins. To identify potential direct targets of RsaOI among candidates identified by proteomic approach, we conducted *in silico* analysis using software tools such as CopraRNA and RNA predator, which predict sRNA-mRNA interactions (43, 44). These software tools generated a list of putative sRNA targets based on the likelihood of direct interaction with RsaOI through sequence complementarity, while also considering the secondary structure of both interacting partners. We focused on predicted targets that overlapped between the *in-silico* predictions and our proteomic data. Notably, we identified 18 shared mRNA targets: 9 predicted by CopraRNA and 9 by RNApredator (Figure 4B and Supplementary Figure 10A). Interestingly, among these potential targets, *vraSR* mRNA, encoding the transcriptional regulator of *rsaOI*, was predicted to interact with RsaOI, as suggested by CopraRNA (Figure 4B). The predicted interaction is located in *vraS* coding sequence, 87 nucleotides upstream of translational initiation site of *vraR* (Supplementary Figure 10B). Despite the predicted RsaOI-*vraSR* mRNA interaction, we did not identify a mechanism responsible for *vraSR* regulation.

Regarding potential regulation of VraSR TCS by RsaOI, we hypothesized that differences in glycopeptide survival could result from RsaOI mediated inhibition of VraR protein level. To test this, we conducted vancomycin survival assay using *vraR* deletion strains, with or without RsaOI expression driven by a constitutive *amiA* promoter (Supplementary Figure 11). Since VraR is a transcriptional regulator of RsaOI, the use of this promoter was essential. The deletion of *vraR* significantly increases bacterial sensitivity to vancomycin, as previously described. Notably, *rsaOI* expression in a *vraR* deletion mutant further affects survival, suggesting that RsaOI influences vancomycin tolerance through the regulation of additional targets.

Remarkably, the Venn diagram analysis revealed a single shared target between both bioinformatics tools and our proteomics data: *lacD* (SAOUHSC_02452), part of the *lac* operon (Figure 4B and 4C). The *lac* operon is composed by seven gene (*lacABCDFEG*) involved in galactose metabolism through the tagatose pathway. The interaction between *lacD* mRNA and RsaOI involved 25 nucleotides for base-pairing (Figure 4C). The predicted interaction engaged the RBS and start codon of *lacD* and is conserved in other staphylococcal species, *S. argentus* and *S. chweitzeri*, where *rsaOI* gene is also present (Supplementary Figure 12). Altogether, the compilation of *in vivo* data revealing that presence

of RsaOI reduces the LacD protein levels and *in silico* predictions of RsaOI binding at the *lacD* RBS, suggested a post-transcriptional mechanism of *lacD* regulation.

Altogether, the *in vivo* data showing that RsaOI reduces LacD protein levels, along with *in silico* predictions of RsaOI binding at the *lacD* RBS, suggest a post-transcriptional mechanism for *lacD* regulation.

RsaOI controls expression of *lacD* at translational level

We focused our next investigations on regulation of *lacD*. Since RsaOI was predicted to bind the mRNA of *lac* transcript in the region of ribosome binding site of *lacD*, we evaluated the formation of the RsaOI-*lacD* mRNA duplex using EMSA (Electrophoretic Mobility Shift Assay). To do this, we produced a 250-nucleotides-long mRNA fragment of *lac* mRNA containing 108 and 142 nucleotides up and downstream of *lacD* start codon, respectively, that includes predicted RsaOI binding site. RsaOI was able to bind to the *lacD* mRNA fragment (Figure 5A), with 50% of formation of complex at 50 pmol of *lacD* mRNA (Figure 5B). The specificity of this interaction was confirmed by the lack of binding interference from an excess of yeast tRNA (Figure 5A). We constructed a mutant version of RsaOI (RsaOI-mut), which lacks 30 nucleotides at the predicted interaction site with *lacD* mRNA. RsaOI-mut was unable to form a duplex with *lacD* mRNA, indicating that these nucleotides are crucial for direct interaction (Figure 5A and 5B).

Next, we evaluated the effect of RsaOI binding to the *lacD* RBS on *lacD* regulation *in vivo*. For this, the sequence of *lacD* mRNA used for *in vitro* study of interaction was fused in-frame with GFP reporter and positioned under the control of the constitutive *tufA* promoter to bypass the regulation on transcriptional level. Plasmid expressing *lacD*-GFP reporter fusion was introduced in both the HG003 strain and its isogenic derivative Δ*rsaOI*. *rsaOI* was expressed under control of its native promoter (pICS3-*rsaOI*) or constitutive promoter (pICS3-*PamiA*-*rsaOI*). The effects of RsaOI on *lacD* expression were evaluated by measuring fluorescence intensity through quantitative microplate assays. To permit *rsaOI* expression under control of its native promoter, we cultured the cells in BHI medium, which allow acidification of the medium (Supplementary Figure 13). Expression of *rsaOI* reduced the fluorescence produced by *S. aureus* cells containing *lacD*-GFP translational fusion (Figure 5C). The decrease of fluorescence was correlated with *rsaOI* expression level, since the high level of *rsaOI* expressed from a strong *amiA* promoter resulted in more pronounced fluorescent inhibition. Moreover, the expression of *rsaOI*-mut allele (Supplementary Figure 13) incapable for *lacD* mRNA binding *in vitro* (p-*rsaOI-mut*) had no effect over the fluorescence, thereby confirming the specificity of the regulation. To note, that for unknown reasons, we were unable to introduce the vector expressing the *rsaOI*-mut under the control of the constitutive *amiA* promoter in *S. aureus*. To determine whether RsaOI affects *lacD* by altering its mRNA levels, we measured the amount of *lacD-gfp* mRNA

depending on RsaOI expression (Figure 5D). No significant effect of RsaOI on mRNA levels was noticed suggesting that RsaOI acts through an antisense mechanism, leading to translational repression of *lacD*.

RsaOI impairs galactose utilization in *S. aureus*

Since *S. aureus* can metabolize galactose exclusively *via* tagatose pathway (45), which involves the *lac* operon (Figure 6A), and regarding the effect of RsaOI on *lacD* expression, we evaluated an impact of RsaOI on bacterial growth in medium supplemented with galactose. We used NZM medium, which lacks external sugar, and NZM supplemented with either glucose or galactose (Figure 6B). In these media, we compared the growth of the *S. aureus* HG003 wild type (WT), a strain lacking *rsaOI* (Δ*rsaOI*), and a strain that constitutively expresses *rsaOI* in a condition-independent manner (Δ*rsaOI/p-PamiA-rsaOI*) (Figure 6B). All strains showed similar growth in NZM alone. Additionally, the supplementation with glucose significantly enhanced growth of all strains. However, when galactose was added, we observed differences in growth depending on *rsaOI*. Indeed, galactose improved the growth of both, the WT and Δ*rsaOI* strains. In contrast, the strain constitutively expressing RsaOI exhibited no growth improvement with galactose compared to NZM alone (Figure 6B). This suggests that expression of RsaOI inhibits galactose utilization likely due to the repression of the *lac* operon.

Impact of unrestrained expression of the *lac* operon on *S. aureus* cell wall morphology

We questioned whether disruptions in *lac* operon expression might impact cell envelope and morphology of *S. aureus*. To explore this, we examined the morphology of *S. aureus* strains with altered *lac* operon expression. Specifically, we analyzed a *lacD*-deleted strain as well as a strain lacking the transcriptional repressor *lacR*, resulting in consistently high *lac* operon expression levels (Figure 7A and 7B). The expression of the *lac* operon in the strain deleted for *lacR* was verified by both qPCR and a promoter fusion of *lac* with the fluorescent GFP protein. In both cases, our results confirmed a strong expression of the *lac* operon in the absence of its transcriptional regulator, validating the strain construction and its role in regulation (Figure 7A and 7B)

Both the Δ*lacD* and Δ*lacR* strains as well as wild-type HG003 strain were grown in rich BHI medium and visualized by electron microscopy. Images showed no significant differences in cell wall structure or cell size between the HG003 and Δ*lacD* strains (Figure 7C). However, the Δ*lacR* strain displayed an abnormal morphology and thickened cell wall compared to the other two strains. These results suggest that dysregulation of *lac* operon expression can lead to abnormal cell phenotypes and

morphological changes. This underscores the importance of tightly controlled *lac* operon expression for normal bacterial growth and cell wall integrity.

DISCUSSION

Acid stress is a common challenge encountered by *S. aureus* throughout its life cycle. This stress can be either endogenous, triggered by sugar metabolism, or exogenous, such as exposure to host defences. To counteract the deleterious effect of pH lowering, *S. aureus* utilizes specific mechanisms and alters its transcriptome by upregulating the acid resistance regulon. This includes genes involved in urea degradation, amino acid uptake, or factors that modify the membrane charge (2). It is well established that the method of acidification strongly influences the bacterial response, depending on the type of acid used as well as the time of exposure (2).

Our study examined gene expression changes in response to strong acid stress. In addition to identifying genes linked to the characteristic acid stress response regulon, transcriptomic analysis revealed a small RNA, RsaOI, that accumulated significantly under acidic pH conditions. The expression of *rsaOI* was induced by low pH, regardless of either inorganic or organic acid were used and whether the acidification is caused by external acid or results from glucose metabolisms. sRNAs are an integral part of the control network that modulates gene expression, particularly in response to specific growth and stress conditions, through various mechanisms, often affecting transcription, translation, and mRNA stability in their targets (16). This study aimed to position RsaOI within the regulatory framework by identifying the regulator responsible for controlling its expression and analyzing its targetome.

The *rsaOI* is highly conserved in the core genomes of *S. aureus* strains, and found in different coagulase negatives staphylococcal species. In *S. aureus*, the *rsaOI* gene is situated between the *proP* gene, which encodes an osmolyte transporter facilitating bacterial adaptation to osmotic stress, and the *vraABC* operon, involved in fatty acid metabolism (Figure 1B)(32, 33). The *vraABC* operon was shown to be upregulated in staphylococcal strains with increased resistance to vancomycin, while the *vraX* gene is part of the cell wall stress regulon that contributes to glycopeptide resistance (33). The genomic environment surrounding *rsaOI* highlights a hotspot for genes specialized in responding to environmental stress.

We identified a mechanism responsible for RsaOI accumulation and have shown that a response regulator VraR activates the *rsaOI* promoter in response to pH decrease. VraSR is homologous to the LiaSR TCSs found in other Gram-positive bacteria, including *B. subtilis*, *Streptococcus mutans*, and *Enterococcus faecalis* (46, 47). These conserved TCSs sense disruptions in the cell wall caused by cell wall-targeting antibiotics (40, 48). Upon activation, VraS phosphorylates VraR, the response regulator,

which subsequently fine-tunes the expression of the cell wall stress stimulon. This stimulon encompasses genes involved in cell wall biosynthesis and remodeling, enabling an adaptive response to maintain cell envelope integrity under stress (48). However, the stimulus as well as the composition of VraSR regulons vary extensively and appear to be dependent upon the strains and experimental procedures used (48, 49). In other Gram-positive bacteria, the *liaSR* homologs have already been shown to be implicated in acid stress response (50). In *S. aureus*, initially, VraSR system was shown to be induced by a number of cell wall antibiotics, including vancomycin, teicoplanin and β-lactams, but not by general stresses, such as acid pH (40, 48). However, recent study has demonstrated that RsaOI affects the growth of *S. aureus* at low pH (8). In line with this data, our findings demonstrate a slight induction in *vraRS* expression. Furthermore, our transcriptome and consequent analyses demonstrated that two known direct VraSR targets, *cwrA* and *vraX* (51, 52), are significantly upregulated under acidic conditions in a VraSR-dependent manner. Therefore, here, we report that low pH induces VraSR-activated response leading to induction of expression of several targets, such as *cwrA* and *vraX*, of VraSR regulon. In addition, we identified *rsaOI* as a new part of VraSR regulon. Particularly, the genomic proximity of *rsaOI* and *vraX*, along with their coordinated expression profile, suggests a potential gene platform responding to stress under VraSR control.

Notably, acidic stress led to only partial induction of the VraSR-regulated stimulon. Our analysis, along with previously published data on the transcriptional response to acid stress, did not reveal the full set of VraSR targets that are typically induced in response to cell wall-inhibitory antibiotics (40, 53). The overlap between the acid stress regulon and other stimulons has been documented and appears to be conserved across different species, with a significant number of genes induced under both stress conditions (5, 54). However, the mechanism underlying the selective activation of specific genes within the regulon remains unknown. This variation in transcriptomic responses emphasizes the existence of a core regulon and an accessory regulon, commonly associated with many transcriptional regulators and previously described in different bacteria species (55, 56). Interestingly, RsaOI was previously shown to accumulate in the presence of vancomycin, underscoring the crosstalk between the cell wall stress regulon induced by cell wall-acting antibiotics and the acid stress regulon (36, 37). Consistent with these findings and the inclusion of RsaOI within the cell wall stress regulon, we demonstrated that RsaOI influences bacterial susceptibility to glycopeptide antibiotics.

To identify targets of RsaOI, we compared the proteomes of strains with varying RsaOI expression levels. Interestingly, among the proteins whose levels depend on RsaOI, a considerable number are involved in carbon metabolism. Levels of proteins such as PckA, Fda, and LacD were increased in the *rsaOI* deletion strain, indication that RsaOI inhibits their expression. A recent study linked RsaOI to carbon metabolic regulation through its influence on the expression of *ptsH*, which encodes protein Hpr, involved in catabolite repression by interacting with CcpA (36). However, in our study, Hpr protein levels remained unchanged regardless of *rsaOI* expression. This indicates that the observed

variations in the levels of metabolism-related proteins in our study are independent of Hpr. The identification of numerous metabolism-related proteins influenced by RsaOI supports role of this sRNA in metabolic regulation.

To identify the direct targets of RsaOI within our proteomic data, we integrated our findings with an *in silico* analysis to predict direct sRNA-mRNA interactions. This approach highlighted *lacD* as a potential direct target, with a predicted interaction that is conserved not only among *S. aureus* strains but also in coagulase-negative staphylococci such as *S. xylosus* and *S. schweitzer*i. Our experiences show that RsaOI inhibits the expression of *lacD* by antisense pairing to its ribosome binding site (RBS), resulting in reduced LacD protein production. A deletion of the region of RsaOI involved in binding to *lacD* mRNA disrupts complex formation, resulting to the loss of regulation *in vivo*. Through downregulating the expression of *lacD*, encoding for tagatose 1,6-diphosphate aldolase, an enzyme involved in the tagatose pathway, RsaOI modulates galactose metabolism. This pathway is the sole means for galactose degradation in *S. aureus*, consequently, overexpression of RsaOI leads to a complete loss of bacterium ability to metabolize this sugar. Similarly, Spot 42 sRNA in *E. coli* has been linked to galactose metabolism through direct binding to the *galETKM* operon mRNA (57). This interaction inhibits the translation of GalK, preventing metabolization of galactose.

By regulating *lacD*, RsaOI could be responsible for the connection between cell wall stress response induced by VraSR and galactose metabolism. Moreover, our studies have demonstrated that removal of inhibition of the *lac* operon in *S. aureus* impacts cell morphology and cell envelope structure. In Gram-positive bacteria possessing the Leloir pathway, galactose is metabolized through this pathway leading to the formation of intermediates, UDP-glucose and UDP-galactose, which serve as precursors for cell wall biosynthesis and sugar substitution of lipoteichoic acid (LTA) (58). In *S. aureus*, which does not possess the Leloir pathway, the tagatose pathway encoded by *lac* operon, is the exclusive metabolic route to breakdown galactose into derivates, that can be used for energy and biosynthesis. By this pathway galactose can be converted into tagatose-6-phosphate, which is further processed to produce glyceraldehyde-3-phosphate and dihydroxyacetone phosphate. These intermediates enter central metabolic pathways (like glycolysis), contributing to the pool of building blocks needed for synthesizing essential biomolecules, including the peptidoglycan layers of the cell wall. Disruptions in central metabolism can lead to changes in peptidoglycan synthesis, impacting cell wall thickness and stability (59). Moreover, the enzyme tagatose-1,6-bisphosphate aldolase, encoded by *lacD*, although exhibits its highest affinity for D-tagatose-1,6-bisphosphate but can also use other D-hexose bisphosphate stereoisomers as substrates, including sorbose bisphosphate, psicose bisphosphate, and fructose bisphosphate (60). Fructose monophosphate participates in the formation of UDP-GlcNAc, which is also a precursor for the cell wall (61). We hypothesize that the *lac* operon of *S. aureus* contributes to the formation of intermediates for the cell wall, which explains the severely disrupted morphology observed when its expression is dysregulated. Notably, several studies have reported links

between the *lac* operon and cell wall-acting antibiotics, suggesting peptidoglycan modification; however, the exact mechanisms are yet to be elucidated (62–64).

In *S. aureus*, *s*RNAs were shown to play a role in the response to variety of environmental stresses, including pH changes, osmotic stress, and nutrient limitations (65). Some of them, such as SprX and 6S RNA, have been found to influence the bacterial susceptibility to antibiotics (27, 66). Here we report RsaOI as an environment-sensitive sRNA, induced through VraSR two-component system under cell wall stress, whether from glycopeptide exposure or environmental acidification. RsaOI modulates bacterial metabolism by regulating the tagatose pathway, whose overproduction leads to abnormal cell wall morphology. Therefore, this study highlights the important role of sRNAs in maintaining cellular integrity and the overlapping responses to multiple cell wall-related stress and carbon metabolism.

ACKNOWLEDGEMENTS

S.M. thanks the Région Normandie for the engineer financial support. Europe gets involved in Normandy with European Regional Development Fund (ERDF). This project has received funding from the European Union's Horizon 2020 research and innovation programme under the Marie Skłodowska-Curie grant agreement No 101034329. This project has received funding from the Normandy Region under the WINNINGNormandy program. MG, HR, AR, and SC thanks Rennes university for financial support (from "Défis émergents" program).

REFERENCES

1. Lowy,F.D. (1998) Staphylococcus aureus infections. *N Engl J Med*, **339**, 520–532.

2. Zhou,C. and Fey,P.D. (2020) The acid response network of Staphylococcus aureus. *Curr Opin Microbiol*, **55**, 67–73.

3. Wu,H., Zhang,Y., Li,L., Li,Y., Yuan,L., E,Y. and Qiao,J. (2022) Positive regulation of the DLT operon by TCSR7 enhances acid tolerance of Lactococcus lactis F44. *J Dairy Sci*, **105**, 7940–7950.

4. Boyd,D.A., Cvitkovitch,D.G., Bleiweis,A.S., Kiriukhin,M.Y., Debabov,D.V., Neuhaus,F.C. and Hamilton,I.R. (2000) Defects in D-alanyl-lipoteichoic acid synthesis in Streptococcus mutans results in acid sensitivity. *J Bacteriol*, **182**, 6055–6065.

5. Weinrick,B., Dunman,P.M., McAleese,F., Murphy,E., Projan,S.J., Fang,Y. and Novick,R.P. (2004) Effect of mild acid on gene expression in Staphylococcus aureus. *J Bacteriol*, **186**, 8407–8423.

6. Grosser,M.R., Paluscio,E., Thurlow,L.R., Dillon,M.M., Cooper,V.S., Kawula,T.H. and Richardson,A.R. (2018) Genetic requirements for Staphylococcus aureus nitric oxide resistance and virulence. *PLoS Pathog*, **14**, e1006907.

684 7. Rode,T.M., Møretrø,T., Langsrud,S., Langsrud,O., Vogt,G. and Holck,A. (2010) Responses of
685 Staphylococcus aureus exposed to HCl and organic acid stress. *Can J Microbiol*, **56**, 777–792.

686 8. Beetham,C.M., Schuster,C.F., Kviatkovski,I., Santiago,M., Walker,S. and Gründling,A. (2024)
687 Histidine transport is essential for the growth of Staphylococcus aureus at low pH. *PLoS Pathog*, **20**,
688 e1011927.

689 9. Alreshidi,M.M., Dunstan,R.H., Macdonald,M.M., Gottfries,J. and Roberts,T.K. (2019) The Uptake
690 and Release of Amino Acids by Staphylococcus aureus at Mid-Exponential and Stationary Phases and
691 Their Corresponding Responses to Changes in Temperature, pH and Osmolality. *Front Microbiol*, **10**,
692 3059.

693 10. Cunin,R., Glansdorff,N., Piérard,A. and Stalon,V. (1986) Biosynthesis and metabolism of arginine
694 in bacteria. *Microbiol Rev*, **50**, 314–352.

695 11. Anderson,K.L., Roux,C.M., Olson,M.W., Luong,T.T., Lee,C.Y., Olson,R. and Dunman,P.M. (2010)
696 Characterizing the effects of inorganic acid and alkaline shock on the Staphylococcus aureus
697 transcriptome and messenger RNA turnover. *FEMS Immunol Med Microbiol*, **60**, 208–250.

698 12. Bore,E., Langsrud,S., Langsrud,Ø., Rode,T.M. and Holck,A. (2007) Acid-shock responses in
699 Staphylococcus aureus investigated by global gene expression analysis. *Microbiology (Reading)*, **153**,
700 2289–2303.

701 13. Zhou,C., Bhinderwala,F., Lehman,M.K., Thomas,V.C., Chaudhari,S.S., Yamada,K.J., Foster,K.W.,
702 Powers,R., Kielian,T. and Fey,P.D. (2019) Urease is an essential component of the acid response
703 network of Staphylococcus aureus and is required for a persistent murine kidney infection. *PLoS*
704 *Pathog*, **15**, e1007538.

705 14. Chaili,S., Cheung,A.L., Bayer,A.S., Xiong,Y.Q., Waring,A.J., Memmi,G., Donegan,N., Yang,S.-J. and
706 Yeaman,M.R. (2016) The GraS Sensor in Staphylococcus aureus Mediates Resistance to Host Defense
707 Peptides Differing in Mechanisms of Action. *Infect Immun*, **84**, 459–466.

708 15. Flannagan,R.S., Kuiack,R.C., McGavin,M.J. and Heinrichs,D.E. (2018) Staphylococcus aureus Uses
709 the GraXRS Regulatory System To Sense and Adapt to the Acidified Phagolysosome in Macrophages.
710 *mBio*, **9**, e01143-18.

711 16. Nitzan,M., Rehani,R. and Margalit,H. (2017) Integration of Bacterial Small RNAs in Regulatory
712 Networks. *Annu Rev Biophys*, **46**, 131–148.

713 17. Beisel,C.L. and Storz,G. (2010) Base pairing small RNAs and their roles in global regulatory
714 networks. *FEMS Microbiol Rev*, **34**, 866–882.

715 18. Storz,G., Vogel,J. and Wassarman,K.M. (2011) Regulation by small RNAs in bacteria: expanding
716 frontiers. *Mol Cell*, **43**, 880–891.

717 19. Waters,L.S. and Storz,G. (2009) Regulatory RNAs in bacteria. *Cell*, **136**, 615–628.

718 20. Wagner,E.G.H. and Romby,P. (2015) Small RNAs in bacteria and archaea: who they are, what they
719 do, and how they do it. *Adv Genet*, **90**, 133–208.

720 21. Sassi,M., Augagneur,Y., Mauro,T., Ivain,L., Chabelskaya,S., Hallier,M., Sallou,O. and Felden,B.
721 (2015) SRD: a Staphylococcus regulatory RNA database. *RNA*, **21**, 1005–1017.

722 22. Monk,I.R., Tree,J.J., Howden,B.P., Stinear,T.P. and Foster,T.J. (2015) Complete Bypass of
723 Restriction Systems for Major Staphylococcus aureus Lineages. *mBio*, **6**, e00308-00315.

724 23. Le Huyen,K.B., Gonzalez,C.D., Pascreau,G., Bordeau,V., Cattoir,V., Liu,W., Bouloc,P., Felden,B. and
725 Chabelskaya,S. (2021) A small regulatory RNA alters Staphylococcus aureus virulence by titrating
726 RNAIII activity. *Nucleic Acids Res*, **49**, 10644–10656.

727 24. Fey,P.D., Endres,J.L., Yajjala,V.K., Widhelm,T.J., Boissy,R.J., Bose,J.L. and Bayles,K.W. (2013) A
728 genetic resource for rapid and comprehensive phenotype screening of nonessential Staphylococcus
729 aureus genes. *mBio*, **4**, e00537-00512.

730 25. Ivain,L., Bordeau,V., Eyraud,A., Hallier,M., Dreano,S., Tattevin,P., Felden,B. and Chabelskaya,S.
731 (2017) An in vivo reporter assay for sRNA-directed gene control in Gram-positive bacteria: identifying
732 a novel sRNA target in Staphylococcus aureus. *Nucleic Acids Res*, **45**, 4994–5007.

733 26. Mauro,T., Rouillon,A. and Felden,B. (2016) Insights into the regulation of small RNA expression:
734 SarA represses the expression of two sRNAs in Staphylococcus aureus. *Nucleic Acids Res*, **44**, 10186–
735 10200.

736 27. Eyraud,A., Tattevin,P., Chabelskaya,S. and Felden,B. (2014) A small RNA controls a protein
737 regulator involved in antibiotic resistance in Staphylococcus aureus. *Nucleic Acids Res*, **42**, 4892–
738 4905.

739 28. Xue,T., You,Y., Hong,D., Sun,H. and Sun,B. (2011) The Staphylococcus aureus KdpDE two-
740 component system couples extracellular K+ sensing and Agr signaling to infection programming.
741 *Infect Immun*, **79**, 2154–2167.

742 29. Bohn,C., Rigoulay,C., Chabelskaya,S., Sharma,C.M., Marchais,A., Skorski,P., Borezée-Durant,E.,
743 Barbet,R., Jacquet,E., Jacq,A., *et al.* (2010) Experimental discovery of small RNAs in Staphylococcus
744 aureus reveals a riboregulator of central metabolism. *Nucleic Acids Res*, **38**, 6620–6636.

745 30. Mäder,U., Nicolas,P., Depke,M., Pané-Farré,J., Debarbouille,M., van der Kooi-Pol,M.M., Guérin,C.,
746 Dérozier,S., Hiron,A., Jarmer,H., *et al.* (2016) Staphylococcus aureus Transcriptome Architecture:
747 From Laboratory to Infection-Mimicking Conditions. *PLoS Genet*, **12**, e1005962.

748 31. Liu,W., Rochat,T., Toffano-Nioche,C., Le Lam,T.N., Bouloc,P. and Morvan,C. (2018) Assessment of
749 Bona Fide sRNAs in Staphylococcus aureus. *Front Microbiol*, **9**, 228.

750 32. Wood,J.M. (1988) Proline porters effect the utilization of proline as nutrient or osmoprotectant
751 for bacteria. *J Membr Biol*, **106**, 183–202.

752 33. Kuroda,M., Kuwahara-Arai,K. and Hiramatsu,K. (2000) Identification of the up- and down-
753 regulated genes in vancomycin-resistant Staphylococcus aureus strains Mu3 and Mu50 by cDNA
754 differential hybridization method. *Biochem Biophys Res Commun*, **269**, 485–490.

755 34. Gardete,S., Wu,S.W., Gill,S. and Tomasz,A. (2006) Role of VraSR in antibiotic resistance and
756 antibiotic-induced stress response in Staphylococcus aureus. *Antimicrob Agents Chemother*, **50**,
757 3424–3434.

758 35. McAleese,F., Wu,S.W., Sieradzki,K., Dunman,P., Murphy,E., Projan,S. and Tomasz,A. (2006)
759 Overexpression of genes of the cell wall stimulon in clinical isolates of Staphylococcus aureus
760 exhibiting vancomycin-intermediate- S. aureus-type resistance to vancomycin. *J Bacteriol*, **188**, 1120–
761 1133.

762 36. Wu,W., Pang,C.N.I., Mediati,D.G. and Tree,J.J. (2024) The functional small RNA interactome
763 reveals targets for the vancomycin-responsive sRNA RsaOI in vancomycin-tolerant Staphylococcus
764 aureus. *mSystems*, **9**, e0097123.

765 37. Howden,B.P., Beaume,M., Harrison,P.F., Hernandez,D., Schrenzel,J., Seemann,T., Francois,P. and
766 Stinear,T.P. (2013) Analysis of the small RNA transcriptional response in multidrug-resistant
767 Staphylococcus aureus after antimicrobial exposure. *Antimicrob Agents Chemother*, **57**, 3864–3874.

768 38. Lu,Y., Chen,F., Zhao,Q., Cao,Q., Chen,R., Pan,H., Wang,Y., Huang,H., Huang,R., Liu,Q., *et al.* (2023)
769 Modulation of MRSA virulence gene expression by the wall teichoic acid enzyme TarO. *Nat Commun*,
770 **14**, 1594.

771 39. Balibar,C.J., Shen,X., McGuire,D., Yu,D., McKenney,D. and Tao,J. (2010) cwrA, a gene that
772 specifically responds to cell wall damage in Staphylococcus aureus. *Microbiology (Reading)*, **156**,
773 1372–1383.

774 40. Kuroda,M., Kuroda,H., Oshima,T., Takeuchi,F., Mori,H. and Hiramatsu,K. (2003) Two-component
775 system VraSR positively modulates the regulation of cell-wall biosynthesis pathway in Staphylococcus
776 aureus. *Mol Microbiol*, **49**, 807–821.

777 41. Renzoni,A., Andrey,D.O., Jousselin,A., Barras,C., Monod,A., Vaudaux,P., Lew,D. and Kelley,W.L.
778 (2011) Whole genome sequencing and complete genetic analysis reveals novel pathways to
779 glycopeptide resistance in Staphylococcus aureus. *PLoS One*, **6**, e21577.

780 42. Sassi,M., Felden,B. and Augagneur,Y. (2014) Draft Genome Sequence of Staphylococcus aureus
781 subsp. aureus Strain HG003, an NCTC8325 Derivative. *Genome Announc*, **2**, e00855-14.

782 43. Wright,P.R., Georg,J., Mann,M., Sorescu,D.A., Richter,A.S., Lott,S., Kleinkauf,R., Hess,W.R. and
783 Backofen,R. (2014) CopraRNA and IntaRNA: predicting small RNA targets, networks and interaction
784 domains. *Nucleic Acids Res*, **42**, W119-123.

785 44. Eggenhofer,F., Tafer,H., Stadler,P.F. and Hofacker,I.L. (2011) RNApredator: fast accessibility-based
786 prediction of sRNA targets. *Nucleic Acids Res*, **39**, W149-154.

787 45. Breidt,F., Hengstenberg,W., Finkeldei,U. and Stewart,G.C. (1987) Identification of the genes for
788 the lactose-specific components of the phosphotransferase system in the lac operon of
789 Staphylococcus aureus. *J Biol Chem*, **262**, 16444–16449.

790 46. Jordan,S., Junker,A., Helmann,J.D. and Mascher,T. (2006) Regulation of LiaRS-dependent gene
791 expression in bacillus subtilis: identification of inhibitor proteins, regulator binding sites, and target
792 genes of a conserved cell envelope stress-sensing two-component system. *J Bacteriol*, **188**, 5153–
793 5166.

794 47. Klinzing,D.C., Ishmael,N., Hotopp,J.C.D., Tettelin,H., Shields,K.R., Madoff,L.C. and Puopolo,K.M.
795 (2013) The two-component response regulator LiaR regulates cell wall stress responses, pili
796 expression and virulence in group B Streptococcus. *Microbiology (Reading)*, **159**, 1521–1534.

797 48. Pietiäinen,M., François,P., Hyyryläinen,H.-L., Tangomo,M., Sass,V., Sahl,H.-G., Schrenzel,J. and
798 Kontinen,V.P. (2009) Transcriptome analysis of the responses of Staphylococcus aureus to
799 antimicrobial peptides and characterization of the roles of vraDE and vraSR in antimicrobial
800 resistance. *BMC Genomics*, **10**, 429.

801 49. Dengler,V., Meier,P.S., Heusser,R., Berger-Bächi,B. and McCallum,N. (2011) Induction kinetics of
802 the Staphylococcus aureus cell wall stress stimulon in response to different cell wall active
803 antibiotics. *BMC Microbiol*, **11**, 16.

804 50. Gong,Y., Tian,X.-L., Sutherland,T., Sisson,G., Mai,J., Ling,J. and Li,Y.-H. (2009) Global
805 transcriptional analysis of acid-inducible genes in Streptococcus mutans: multiple two-component
806 systems involved in acid adaptation. *Microbiology (Reading)*, **155**, 3322–3332.

807 51. Yan,J., Han,D., Liu,C., Gao,Y., Li,D., Liu,Y. and Yang,G. (2017) Staphylococcus aureus VraX
808 specifically inhibits the classical pathway of complement by binding to C1q. *Mol Immunol*, **88**, 38–44.

809 52. Han,W., Xiao,Y., Shen,L., Yuan,X., Yu,J., Gao,H., Hu,R., Shi,J., Wang,B., Zhang,J., *et al.* (2024) The
810 roles of cell wall inhibition responsive protein CwrA in the pathogenicity of Staphylococcus aureus.
811 *Virulence*, **15**, 2411540.

812 53. Boyle-Vavra,S., Yin,S., Jo,D.S., Montgomery,C.P. and Daum,R.S. (2013) VraT/YvqF is required for
813 methicillin resistance and activation of the VraSR regulon in Staphylococcus aureus. *Antimicrob*
814 *Agents Chemother*, **57**, 83–95.

815 54. Utaida,S., Dunman,P.M., Macapagal,D., Murphy,E., Projan,S.J., Singh,V.K., Jayaswal,R.K. and
816 Wilkinson,B.J. (2003) Genome-wide transcriptional profiling of the response of Staphylococcus
817 aureus to cell-wall-active antibiotics reveals a cell-wall-stress stimulon. *Microbiology (Reading)*, **149**,
818 2719–2732.

819 55. Hause,L.L. and McIver,K.S. (2012) Nucleotides critical for the interaction of the Streptococcus
820 pyogenes Mga virulence regulator with Mga-regulated promoter sequences. *J Bacteriol*, **194**, 4904–
821 4919.

822 56. Tribelli,P.M., Lujan,A.M., Pardo,A., Ibarra,J.G., Fernández Do Porto,D., Smania,A. and López,N.I.
823 (2019) Core regulon of the global anaerobic regulator Anr targets central metabolism functions in
824 Pseudomonas species. *Sci Rep*, **9**, 9065.

825 57. Møller,T., Franch,T., Udesen,C., Gerdes,K. and Valentin-Hansen,P. (2002) Spot 42 RNA mediates
826 discoordinate expression of the E. coli galactose operon. *Genes Dev*, **16**, 1696–1706.

827 58. Schneewind,O. and Missiakas,D. (2014) Lipoteichoic acids, phosphate-containing polymers in the
828 envelope of gram-positive bacteria. *J Bacteriol*, **196**, 1133–1142.

829 59. Martínez,B., Rodríguez,A., Kulakauskas,S. and Chapot-Chartier,M.-P. (2020) Cell wall homeostasis
830 in lactic acid bacteria: threats and defences. *FEMS Microbiol Rev*, **44**, 538–564.

831 60. LowKam,C., Liotard,B. and Sygusch,J. (2010) Structure of a class I tagatose-1,6-bisphosphate
832 aldolase: investigation into an apparent loss of stereospecificity. *J Biol Chem*, **285**, 21143–21152.

833 61. Vemula,H., Ayon,N.J. and Gutheil,W.G. (2016) Cytoplasmic peptidoglycan intermediate levels in
834 Staphylococcus aureus. *Biochimie*, **121**, 72–78.

835 62. Thitiananpakorn,K., Aiba,Y., Tan,X.-E., Watanabe,S., Kiga,K., Sato'o,Y., Boonsiri,T., Li,F.-Y.,
836 Sasahara,T., Taki,Y., *et al.* (2020) Association of mprF mutations with cross-resistance to daptomycin
837 and vancomycin in methicillin-resistant Staphylococcus aureus (MRSA). *Sci Rep*, **10**, 16107.

838 63. Li,Y., Chen,L., Zhu,F., Bayer,A.S. and Xiong,Y.Q. (2022) Transcriptome Analyses of Prophage in
839 Mediating Persistent Methicillin-Resistant Staphylococcus aureus Endovascular Infection. *Genes*
840 *(Basel)*, **13**, 1527.

841 64. Shoji,M., Cui,L., Iizuka,R., Komoto,A., Neoh,H., Watanabe,Y., Hishinuma,T. and Hiramatsu,K.
842 (2011) walK and clpP mutations confer reduced vancomycin susceptibility in Staphylococcus aureus.
843 *Antimicrob Agents Chemother*, **55**, 3870–3881.

65. Menard,G., Silard,C., Suriray,M., Rouillon,A. and Augagneur,Y. (2022) Thirty Years of sRNA-Mediated Regulation in Staphylococcus aureus: From Initial Discoveries to In Vivo Biological Implications. *Int J Mol Sci*, **23**, 7346.

66. Esberard,M., Hallier,M., Liu,W., Morvan,C., Bossi,L., Figueroa-Bossi,N., Felden,B. and Bouloc,P. (2022) 6S RNA-Dependent Susceptibility to RNA Polymerase Inhibitors. *Antimicrob Agents Chemother*, **66**, e0243521.

67. Busch,A., Richter,A.S. and Backofen,R. (2008) IntaRNA: efficient prediction of bacterial sRNA targets incorporating target site accessibility and seed regions. *Bioinformatics*, **24**, 2849–2856.

FIGURES LEGENDS

Figure 1: Induced by low pH, *rsaOI* contributes to survival under acidic stress. (**A**) Visualization of the most significantly accumulated mRNAs under acidic (pH 4) and neutral (pH 7) conditions using a Volcano plot. The genes with the highest differential expression are highlighted and labeled. (**B**) Genomic localization of *rsaOI* gene in HG003 strain, situated between *proP* and *vraABC* operon. (**C**) RsaOI expression in response to pH range was analyzed by Northern blot analysis using *rsaOI* specific probe, with tmRNA used as loading control. (**D**) *rsaOI* expression in HG003 WT, Δ*rsaOI* (both carrying pICS3 plasmid; WT/*p* and *ΔrsaOI/p*) or complemented strain (Δ*rsaOI*, carrying pICS3-*rsaOI* plasmid) was analyzed by qPCR, normalized to the control gene *gyrB*, and calculated using $2^{-\Delta\Delta Ct}$ method for relative quantification. (**E**) Strains from pannel (**D**) were cultured in LB medium for 2 hours, then pelleted and resuspended in LB buffered to pH5. After 2 hours at pH5, samples were collected and plated to determine CFU counts. Statistical analysis was conducted using Student's t-test. Error bars represent the average of three independent experiments. Statistical significance is indicated by bars and asterisks as follows: *, P<0.05; **, P<0.05.

Figure 2: VraR affects *rsaOI* expression. (**A**) Fluorescence levels of GFP under control of either *tufA* or *rsaOI* promoters. Cells were grown for 2 hours in LB medium, followed by addition of HCl. All statistical analyses were performed using Student's t-test. Error bars represent the average of three independent experiments. Statistical significance is indicated by bars and asterisks as follows: ***, P<0.001. (**B**) Analysis of *rsaOI* levels in HG003 and Sa564 wild-type strains (WT) and their isogenic mutants. Relative quantification of *rsaOI* expression levels were measured by qPCR, normalized to the control gene *gyrB*, and calculated using $2^{-\Delta\Delta Ct}$ method. (**C**) *rsaOI* expression in WT and in Δ*vraR* mutant according to pH. Cells were cultured in LB medium for 2 hours, then pelleted and resuspended in LB buffered with 100 mM HEPES at pH 5 or pH 7 for 30 minutes. (**D**) Fluorescence levels of GFP under control of *rsaOI* promoter in both HG003 WT and *ΔvraR* strains. Cells were grown for 2 hours in LB medium, followed by HCl addition. Statistical analysis was performed using Student's t-test. Error bars represent the average of three independent experiments. Statistical significance is indicated

by bars and asterisks as follows: ***, P<0.001; ****, P<0.0001. (**E**) Illustration of the induction mediated by the TCS VraSR on the expression of the sRNA *rsaOI* during acid stress or in the presence of the glycopeptide antibiotic vancomycin.

Figure 3: RsaOI modulates *S. aureus* resistance to vancomycin. Ten-fold serial dilutions of overnight cultures of WT HG003, Δ*rsaoi* or complemented strain (Δ*rsaOI/p-rsaOI*) were plated and incubated for 24 hours at 37°C. The 10^{-6} dilution are shown for TSA condition (**A**), and the 10^{-4} dilution for TSA supplemented with 1µg/ml vancomycin (**B**). Diagrams show colony growth quantification. Statistical analysis was performed using Student's t-test. Error bars represent the average of three independent experiments. Statistical significance is indicated by bars and asterisks as follows: ***, P<0.001.

Figure 4: Investigation of the potential direct targets of RsaOI based on *in vivo* proteomic data and *in silico* computational approaches. (**A**) Volcano-plot showing protein relative abundances between the *ΔrsaOI* strain containing a pICS3 vector (*ΔrsaOI/p)* and the complemented strain (*ΔrsaOI/p-ΔrsaOI*) in relation to the *t*-test *p*-value (<0.05). VraR and LacD are significantly more abundant in *ΔrsaOI* strain. (**B**) Venn diagram illustrating the overlap between experimentally identified and *in silico* predicted RsaOI target candidates. Experimentally identified candidates, representing proteins with significantly different abundances, are highlighted in red. The top 100 predicted targets from CopraRNA (43) are shown in blue, while the top 100 predicted by RNA predator (44) are depicted in yellow. Shared targets are represented in the overlapping regions. (**C**) Organization of the *lac* operon in the HG003 strain and the predicted base-pairing interaction between RsaOI and *lac* operon mRNA, generated using IntraRNA software (67). Position +1 corresponds to the start codon of *lacD* and +1 transcription start site for RsaOI.

Figure 5: RsaOI inhibits *lacD* expression. (**A**) Complex formation between RsaOI and *lacD* mRNA was analyzed by native gel retardation assays. Gel shift assays of purified, labeled RsaOI and RsaOI-mut were performed with increasing concentrations of *lacD* mRNA. (**B**) Quantification of complex formation from (A) was performed by ImageQuant Tools 7.0. (**C**) The effect of RsaOI on *lacD* expression was examined using *gfp* gene reporter assay. *S. aureus* WT and Δ*rsaOI* strains containing the pCN33-*PtufA-lacD-gfp* fusion plasmid were co-transformed with pICS3, pICS3 expressing *rsaOI* or *rsaOI-mut* under control of its endogenous promoter, or *rsaOI* under constitutive promoter *amiA*. The fluorescent intensity was measured after 8 hours of growth. Statistical analysis was conducted using a Kruskal-Wallis non-parametric test across all conditions followed by Student's t-test to

determine significant differences among conditions. Error bars represent the average of four independent experiments. Statistical significance is indicated by bars and asterisks as follows: *, P<0.05; **, P<0.01. (**D**) In parallele with the panel (C) experiment, strains were collected and pelleted, and relative quantification of *lacD-gfp* fusion mRNA expression levels were measured by qPCR, normalized to the control gene *gyrB*, and calculated using $2^{-\Delta\Delta Ct}$ method.

Figure 6: *rsaOI* overexpression impairs using of galactose as an external source of carbons. (**A**) Illustration of the tagatose pathway, a metabolic pathway that catabolizes galactose or lactose through the *lac* operon. (**B**) Growth curves of *S. aureus* HG003 WT, Δ*rsaOI*, or complemented strain expressing *rsaOI* under constitutive promoter *amiA* were cultured in NZM media supplemented with glucose or galactose at 11mM. Growth was followed during 16 hours using a Biotek microplate reader. Error bars represent the average of three independent experiments.

Figure 7: *lac* operon impacts cell wall structure. (**A**) Expression levels of the *lac* operon mRNA in the WT strain and Δ*lacR* strain during growth in BHI medium were analyzed by qPCR, normalized to the control gene *gyrB*, and calculated using $2^{-\Delta\Delta Ct}$ method for relative quantification. (**B**) Fluorescence levels of GFP under control of *lac* operon promoter in the WT strain and Δ*lacR* strain. Growth was followed during 14 hours in a BHI medium using a Biotek microplate reader. (**C**) HG003 WT, Δ*lacD*, or Δ*lacR* were cultured in BHI during 6 hours and then collected for transmission electron microscopy (TEM) to observe cell wall alterations.

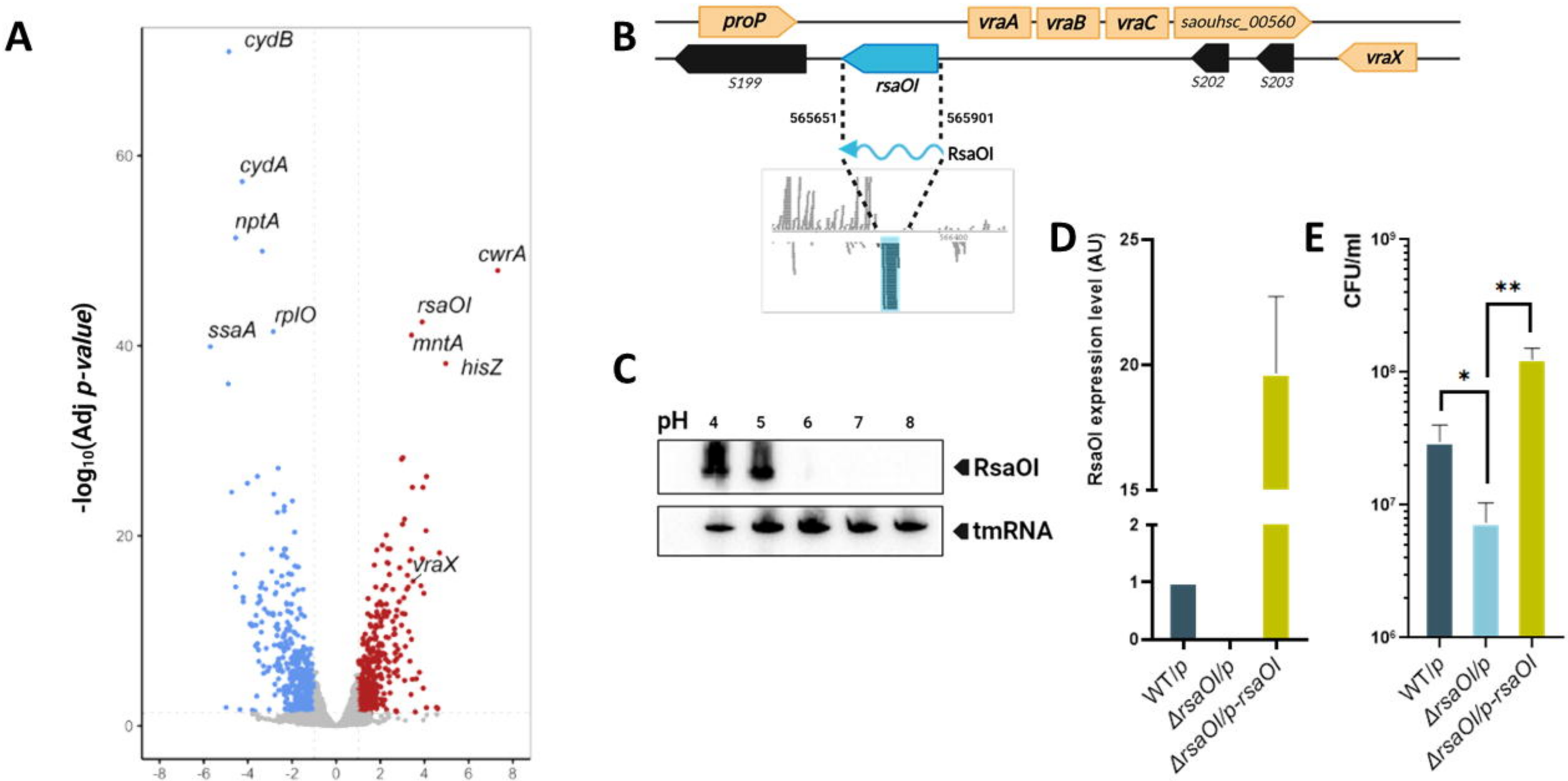
A
cydB
cydA
nptA
cwrA
rsaOI
ssaA
rplO
mntA
hisZ
vraX
-log10(Adj p-value)
log2(FC)
B
proP
vraA
vraB
vraC
saouhsc_00560
vraX
S199
rsaOI
S202
S203
565651
565901
RsaOI
C
pH 4 5 6 7 8
RsaOI
tmRNA
D
RsaOI expression level (AU)
WT/p
ΔrsaOI/p
ΔrsaOI/p-rsaOI
E
CFU/ml
WT/p
ΔrsaOI/p
ΔrsaOI/p-rsaOI

Figure 1

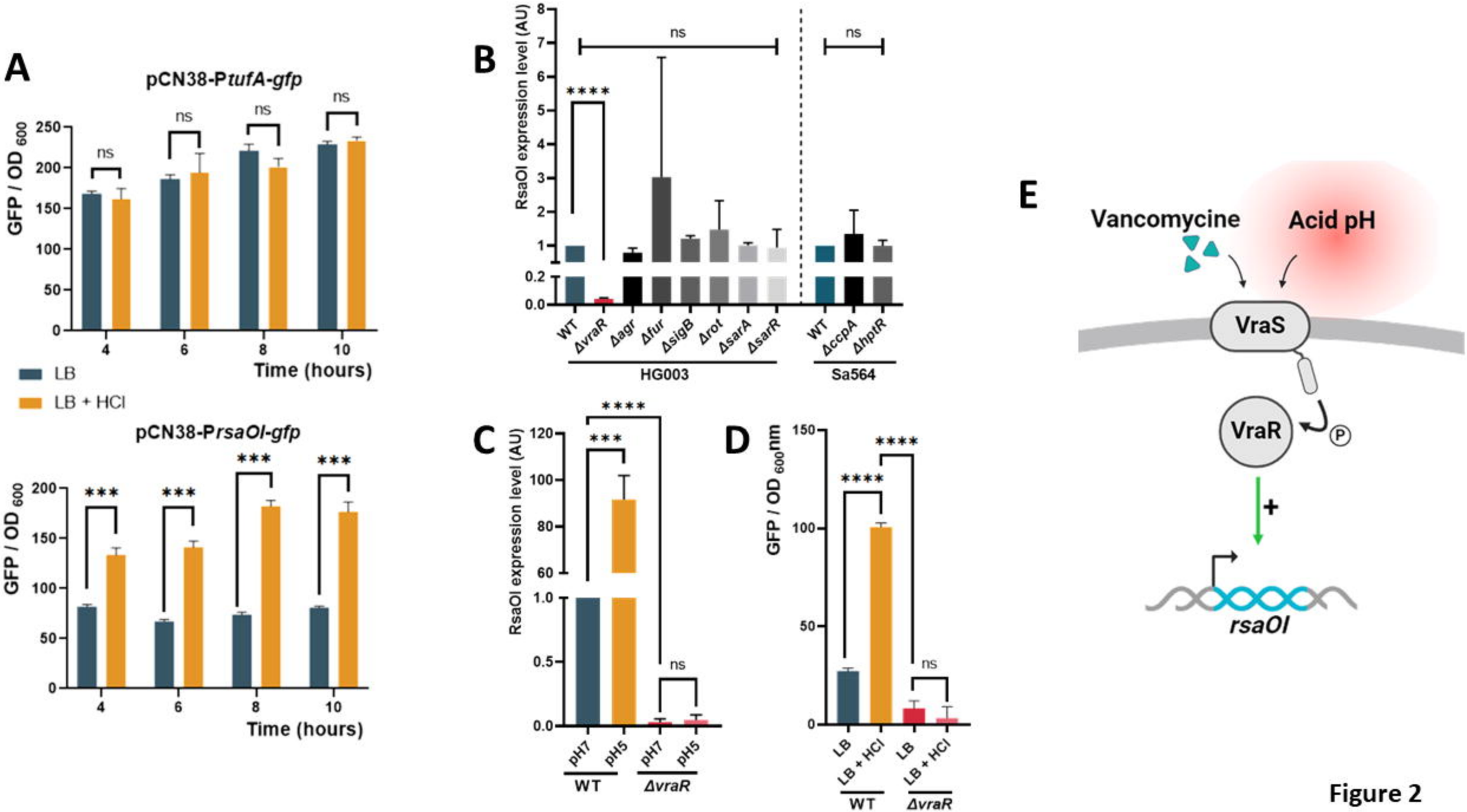
A
pCN38-PtufA-gfp
GFP / OD 600
ns
Time (hours)
LB
LB + HCl
pCN38-PrsaOI-gfp
***
B
RsaOI expression level (AU)
****
ns
WT
ΔvraR
Δagr
Δfur
ΔsigB
Δrot
ΔsarA
ΔsarR
ΔccpA
ΔhptR
HG003
Sa564
C
pH7
pH5
WT
ΔvraR
D
E
Vancomycine
Acid pH
VraS
VraR
P
+
rsaOI

Figure 2

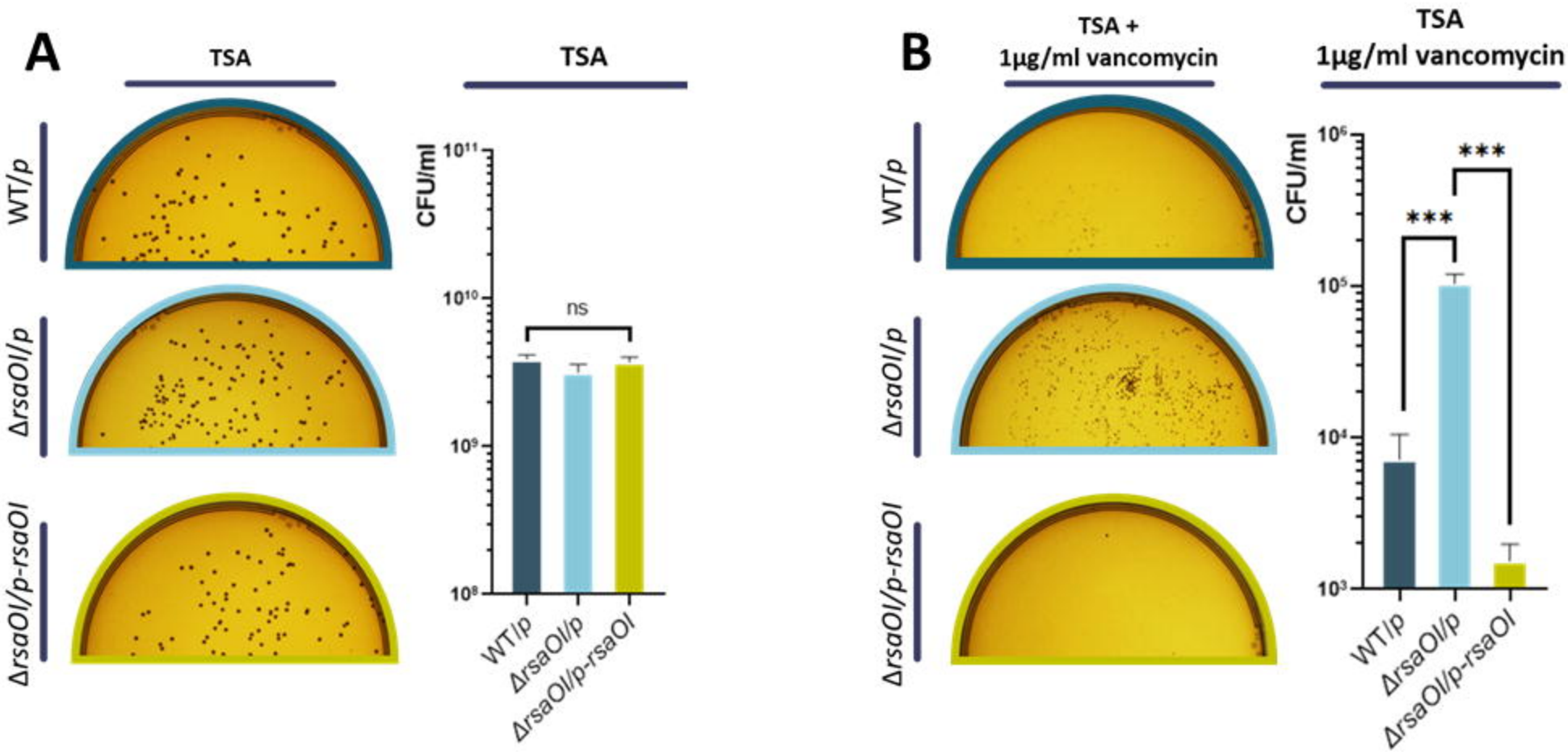
A
TSA
TSA
WT/p
ΔrsaOI/p
ΔrsaOI/p-rsaOI
CFU/ml
10¹¹
10¹⁰
10⁹
10⁸
ns
WT/p
ΔrsaOI/p
ΔrsaOI/p-rsaOI
B
TSA +
1µg/ml vancomycin
TSA
1µg/ml vancomycin
WT/p
ΔrsaOI/p
ΔrsaOI/p-rsaOI
CFU/ml
10⁶
10⁵
10⁴
10³
***
***
WT/p
ΔrsaOI/p
ΔrsaOI/p-rsaOI

Figure 3

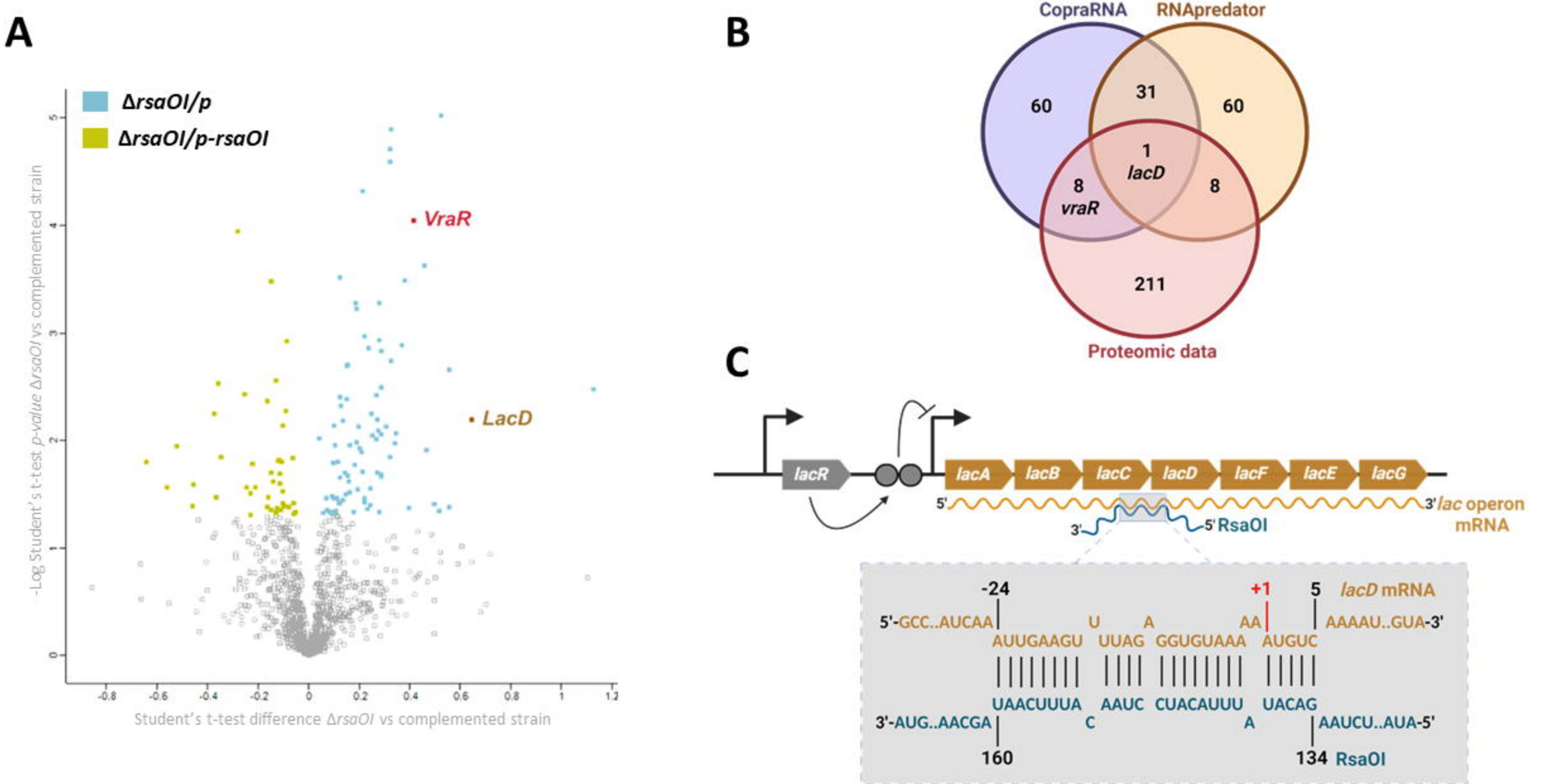
A
ΔrsaOI/p
ΔrsaOI/p-rsaOI
VraR
LacD
-Log Student's t-test p-value ΔrsaOI vs complemented strain
Student's t-test difference ΔrsaOI vs complemented strain
B
CopraRNA
RNApredator
Proteomic data
60
31
60
1
lacD
8
vraR
8
211
C
lacR
lacA
lacB
lacC
lacD
lacF
lacE
lacG
5'
3'
lac operon mRNA
3'
5'
RsaOI
-24
+1
5
lacD mRNA
5'-GCC..AUCAA
AAAAU..GUA-3'
AUUGAAGU
UUAG
GGUGUAAA
AUGUC
UAACUUUA
AAUC
CUACAUUU
UACAG
3'-AUG..AACGA
AAUCU..AUA-5'
160
134
RsaOI

Figure 4

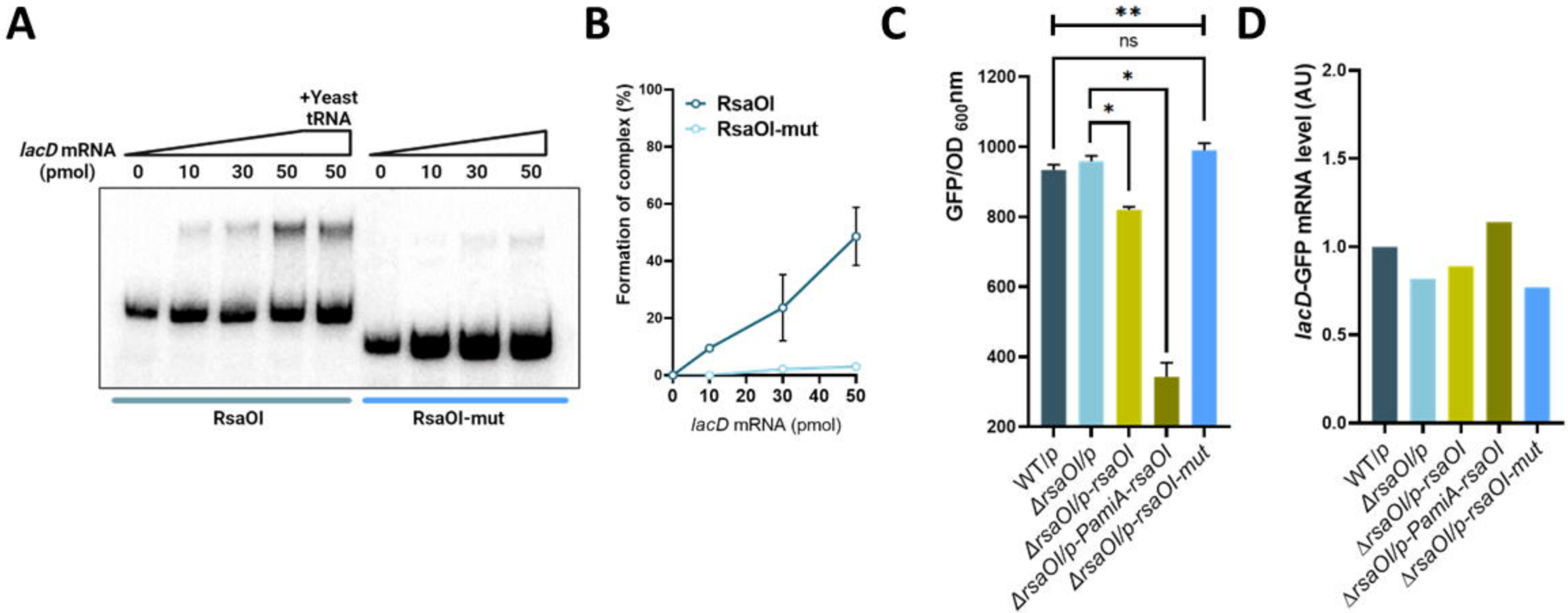
A
+Yeast tRNA
lacD mRNA (pmol)
0 10 30 50 50 0 10 30 50
RsaOI
RsaOI-mut
B
RsaOI
RsaOI-mut
Formation of complex (%)
lacD mRNA (pmol)
C
GFP/OD 600nm
**
ns
*
*
WT/p
ΔrsaOI/p
ΔrsaOI/p-rsaOI
ΔrsaOI/p-PamiA-rsaOI
ΔrsaOI/p-rsaOI-mut
D
lacD-GFP mRNA level (AU)
WT/p
ΔrsaOI/p
ΔrsaOI/p-rsaOI
ΔrsaOI/p-PamiA-rsaOI
ΔrsaOI/p-rsaOI-mut

Figure 5

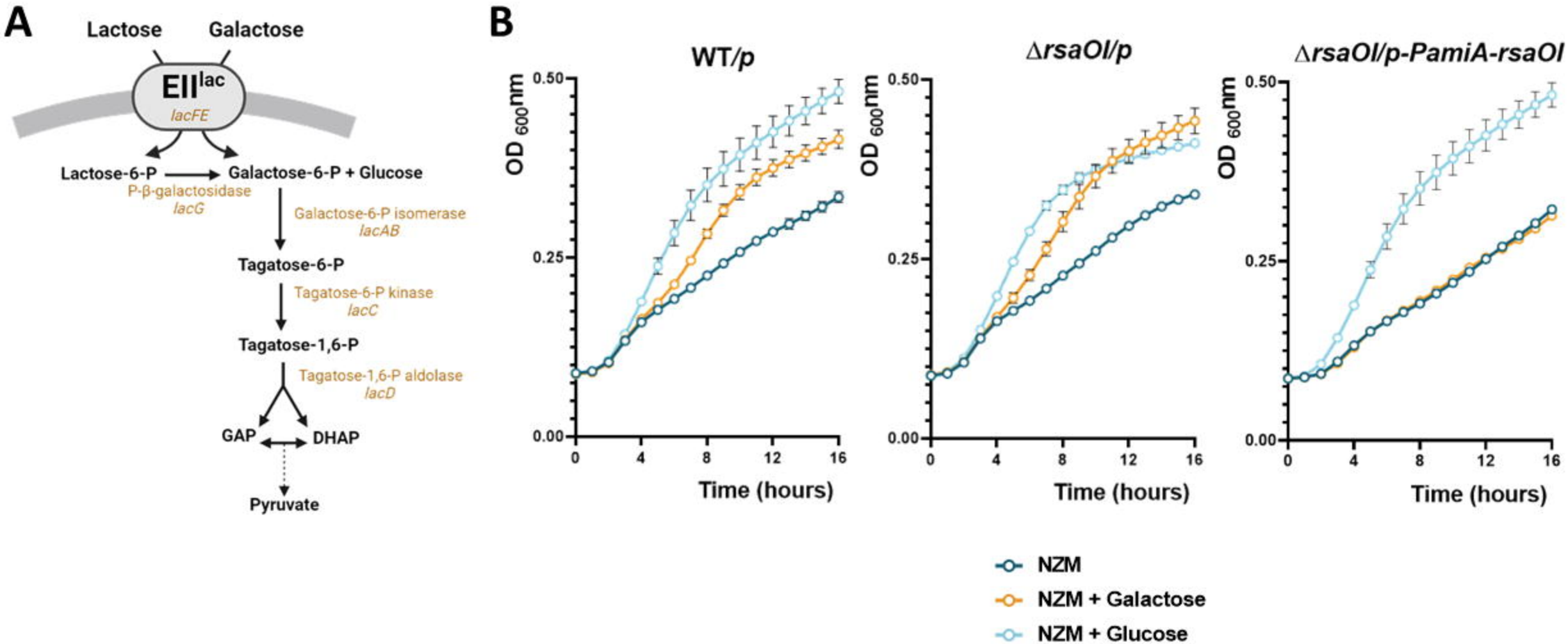
A
Lactose
Galactose
EIIlac
lacFE
Lactose-6-P
Galactose-6-P + Glucose
P-β-galactosidase
lacG
Galactose-6-P isomerase
lacAB
Tagatose-6-P
Tagatose-6-P kinase
lacC
Tagatose-1,6-P
Tagatose-1,6-P aldolase
lacD
GAP
DHAP
Pyruvate
B
WT/p
ΔrsaOI/p
ΔrsaOI/p-PamiA-rsaOI
OD 600nm
0.50
0.25
0.00
0
4
8
12
16
Time (hours)
NZM
NZM + Galactose
NZM + Glucose

Figure 6

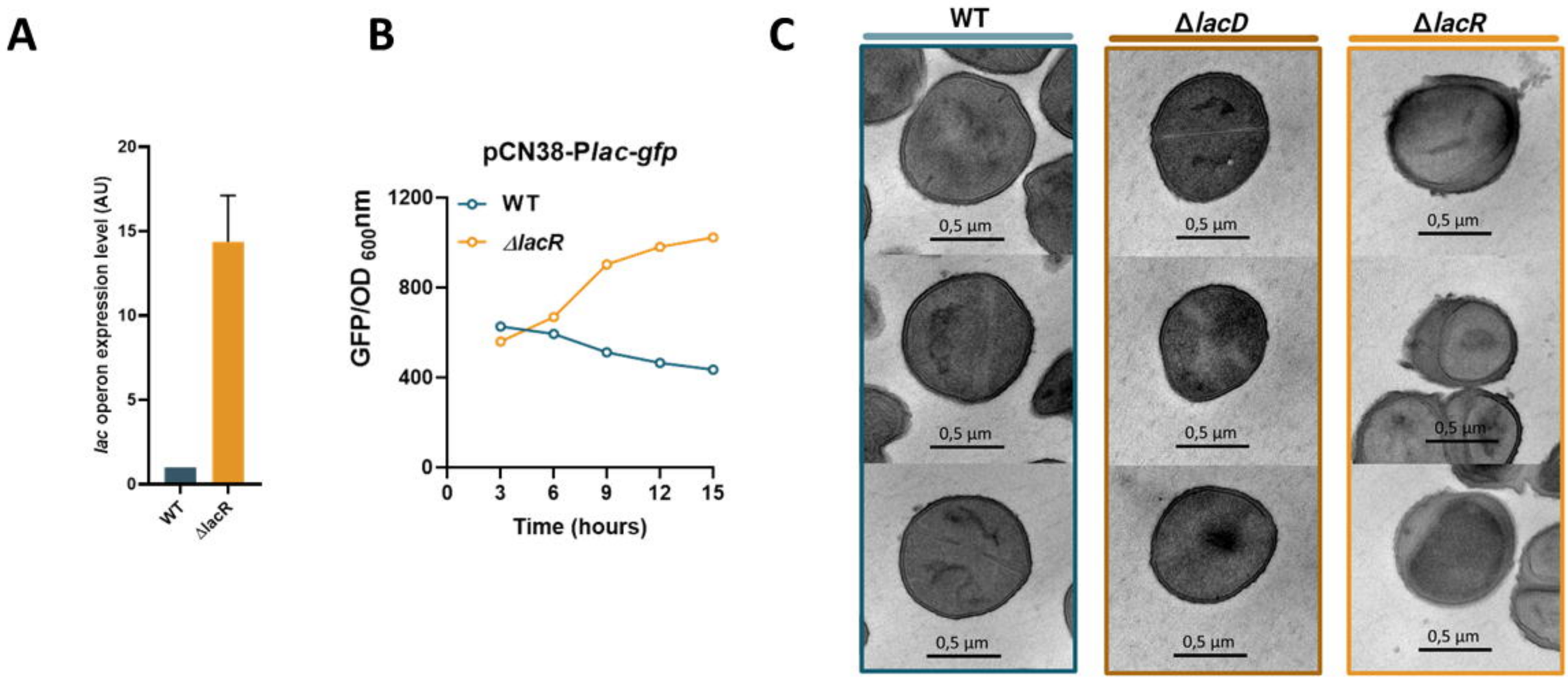
A
lac operon expression level (AU)
20
15
10
5
0
WT
ΔlacR
B
pCN38-Plac-gfp
GFP/OD 600nm
1200
800
400
0
WT
ΔlacR
0
3
6
9
12
15
Time (hours)
C
WT
ΔlacD
ΔlacR
0,5 µm

Figure 7